

27 Abstract

28 Benthic microbial methanogenesis is a known source of methane in marine systems. In most
29 sediments, the majority of methanogenesis is located below the sulfate-reducing zone, as sulfate
30 reducers outcompete methanogens for the major substrates hydrogen and acetate. Coexistence of
31 methanogenesis and sulfate reduction has been shown before and is possible by usage of non-
32 competitive substrates by the methanogens such as methanol or methylated amines. However, the
33 knowledge about magnitude, seasonality and environmental controls on this non-competitive
34 methane production is sparse. In the present study, the presence of methanogenesis within the
35 sulfate reduction zone (SRZ methanogenesis), was investigated in sediments (0-30 centimeters below
36 seafloor, cmbsf) of the seasonally hypoxic Eckernförde Bay, southwestern Baltic Sea. Water column
37 parameters such as oxygen, temperature, and salinity together with porewater geochemistry and
38 benthic methanogenesis rates were determined in the sampling area "Boknis Eck" quarterly from
39 March 2013 to September 2014, to investigate the effect of seasonal environmental changes on the
40 rate and distribution of SRZ methanogenesis, to estimate its potential contribution to benthic
41 methane emissions, and to identify potential methanogenic groups responsible for SRZ
42 methanogenesis. The metabolic pathway of methanogenesis in the presence or absence of sulfate
43 reducers and after the addition of a non-competitive substrate was studied in four experimental
44 setups: 1) unaltered sediment batch incubations (net methanogenesis), 2) ^{14}C -bicarbonate labeling
45 experiments (hydrogenotrophic methanogenesis), 3) manipulated experiments with addition of
46 either molybdate (sulfate reducer inhibitor), 2-bromoethane-sulfonate (methanogen inhibitor), or
47 methanol (non-competitive substrate, potential methanogenesis), 4) addition of ^{13}C -labeled
48 methanol (potential methylotrophic methanogenesis). After incubation with methanol, molecular
49 analyses were conducted to identify key functional methanogenic groups during methylotrophic
50 methanogenesis. To also compare magnitudes of SRZ methanogenesis with methanogenesis below
51 the sulfate reduction zone (> 30 cmbsf), hydrogenotrophic methanogenesis was determined by ^{14}C -
52 bicarbonate radiotracer incubation in samples collected in September 2013.

53 SRZ methanogenesis changed seasonally in the upper 30 cmbsf with rates increasing from March (0.2
54 $\text{nmol cm}^{-3} \text{d}^{-1}$) to November ($1.3 \text{nmol cm}^{-3} \text{d}^{-1}$) 2013 and March ($0.2 \text{nmol cm}^{-3} \text{d}^{-1}$) to September (0.4
55 $\text{nmol cm}^{-3} \text{d}^{-1}$) 2014, respectively. Its magnitude and distribution appeared to be controlled by
56 organic matter availability, C/N, temperature, and oxygen in the water column, revealing higher rates
57 in warm, stratified, hypoxic seasons (September/November) compared to colder, oxygenated
58 seasons (March/June) of each year. The majority of SRZ methanogenesis was likely driven by the
59 usage of non-competitive substrates (e.g., methanol and methylated compounds), to avoid
60 competition with sulfate reducers, as it was indicated by the 1000-3000-fold increase in potential
61 methanogenesis activity observed after methanol addition. Accordingly, competitive

62 hydrogenotrophic methanogenesis increased in the sediment only below the depth of sulfate
63 penetration (> 30 cmbsf). Members of the family *Methanosarcinaceae*, which are known for
64 methylotrophic methanogenesis, were detected by PCR using *Methanosarcinaceae*-specific primers
65 and are likely to be responsible for the observed SRZ methanogenesis.

66 The present study indicates that SRZ methanogenesis is an important component of the benthic
67 methane budget and carbon cycling in Eckernförde Bay. Although its contribution to methane
68 emissions from the sediment into the water column are probably minor, SRZ methanogenesis could
69 directly feed into methane oxidation above the sulfate-methane transition zone.

70 1. Introduction

71 After water vapor and carbon dioxide, methane is the most abundant greenhouse gas in the
72 atmosphere (e.g. Hartmann et al., 2013; Denman et al., 2007). Its atmospheric concentration
73 increased more than 150 % since preindustrial times, mainly through increased human activities such
74 as fossil fuel usage and livestock breeding (Hartmann et al., 2013; Wuebbles & Hayhoe, 2002;
75 Denman et al., 2007). Determining the natural and anthropogenic sources of methane is one of the
76 major goals for oceanic, terrestrial and atmospheric scientists to be able to predict further impacts
77 on the world's climate. The ocean is considered to be a modest natural source for atmospheric
78 methane (Wuebbles & Hayhoe, 2002; Reeburgh, 2007; EPA, 2010). However, research is still sparse
79 on the origin of the observed oceanic methane, which automatically leads to uncertainties in current
80 ocean flux estimations (Bange et al., 1994; Naqvi et al., 2010; Bakker et al., 2014).

81 Within the marine environment, the coastal areas (including estuaries and shelf regions) are
82 considered the major source for atmospheric methane, contributing up to 75 % to the global ocean
83 methane production (Bange et al., 1994). The major part of the coastal methane is produced during
84 microbial methanogenesis in the sediment, with probably only a minor part originating from
85 methane production within the water column (Bakker et al., 2014). However, the knowledge on
86 magnitude, seasonality and environmental controls of benthic methanogenesis is still limited.

87 In marine sediments, methanogenesis activity is mostly restricted to the sediment layers below
88 sulfate reduction, due to the successful competition of sulfate reducers with methanogens for the
89 mutual substrates acetate and hydrogen (H₂) (Oremland & Polcin, 1982; Crill & Martens, 1986;
90 Jørgensen, 2006). Methanogens produce methane mainly from using acetate (acetoclastic
91 methanogenesis) or H₂ and carbon dioxide (CO₂) (hydrogenotrophic methanogenesis). Competition
92 with sulfate reducers can be relieved through usage of non-competitive substrates (e.g. methanol or
93 methylated compounds, methylotrophic methanogenesis) (Cicerone & Oremland, 1988; Oremland &
94 Polcin, 1982). Coexistence of sulfate reduction and methanogenesis has been detected in a few
95 studies from organic-rich sediments, e.g., salt-marsh sediments (Oremland et al., 1982; Buckley et al.,

96 2008), coastal sediments (Holmer & Kristensen, 1994; Jørgensen & Parkes, 2010) or sediments in
97 upwelling regions (Pimenov et al., 1993; Ferdelman et al., 1997; Maltby et al., 2016), indicating the
98 importance of these environments for methanogenesis within the sulfate reduction zone (SRZ
99 methanogenesis). So far, however, environmental controls of SRZ methanogenesis remain elusive.
100 The coastal inlet Eckernförde Bay (southwestern Baltic Sea) is an excellent model environment to
101 study seasonal and environmental controls of benthic SRZ methanogenesis. Here, the muddy
102 sediments are characterized by high organic loading and high sedimentation rates (Whiticar, 2002),
103 which lead to anoxic conditions within the uppermost 0.1-0.2 centimeter below seafloor (cmbsf)
104 (Preisler et al., 2007). Seasonally hypoxic (dissolved oxygen < 63 μ M) and anoxic (dissolved oxygen =
105 0 μ M) events in the bottom water of Eckernförde Bay (Lennartz et al., 2014; Steinle et al., 2017)
106 provide ideal conditions for anaerobic processes at the sediment surface.

107 Sulfate reduction is the dominant pathway of organic carbon degradation in Eckernförde Bay
108 sediments in the upper 30 cmbsf, followed by methanogenesis in deeper sediment layers where
109 sulfate is depleted (>> 30 cmbsf) (Whiticar 2002; Treude et al. 2005; Martens et al. 1998) (Fig. 1). This
110 methanogenesis below the sulfate-methane transition zone (SMTZ) can be intense and often leads to
111 methane oversaturation in the porewater below 50 cm sediment depth, resulting in gas bubble
112 formation (Abegg & Anderson, 1997; Whiticar, 2002; Thießen et al., 2006). Thus, methane is
113 transported from the methanogenic zone (> 30 cmbsf) to the surface sediment by both molecular
114 diffusion and advection via rising gas bubbles (Wever et al., 1998; Treude et al., 2005a). Although
115 upward diffusing methane is mostly retained by anaerobic oxidation of methane (AOM) (Treude et
116 al. 2005), a major part is reaching the sediment-water interface through gas bubble transport
117 (Treude et al. 2005; Jackson et al. 1998), resulting in a supersaturation of the water column with
118 respect to atmospheric methane concentrations (Bange et al., 2010). The Time Series Station “Boknis
119 Eck” in the Eckernförde Bay is a known site of methane emissions into the atmosphere throughout
120 the year due to this supersaturation of the water column (Bange et al., 2010).

121 The source for benthic and water column methane was seen in methanogenesis below the SMTZ (>>
122 30 cmbsf) (Whiticar, 2002), however, coexistence of sulfate reduction and methanogenesis has been
123 postulated (Whiticar, 2002; Treude et al., 2005a). Still, the magnitude and environmental controls of
124 SRZ methanogenesis is poorly understood, even though it may make a measurable contribution to
125 benthic methane emissions given its short diffusion distance to the sediment-water interface (Knittel
126 & Boetius, 2009). Production of methane within the sulfate reduction zone of Eckernförde Bay
127 sediments could further explain peaks of methane oxidation observed in top sediment layers, which
128 was previously attributed to methane transported to the sediment surface via rising gas bubbles
129 (Treude et al., 2005a).

130 In the present study, we investigated sediments from within (< 30 cmbsf, on a seasonal basis) and
131 below the sulfate reduction zone (>> 30 cmbsf, on one occasion), and the water column (on a
132 seasonal basis) at the Time Series Station "Boknis Eck" in Eckernförde Bay, to validate the existence
133 of SRZ methanogenesis and its potential contribution to benthic methane emissions. Water column
134 parameters like oxygen, temperature, and salinity together with porewater geochemistry and
135 benthic methanogenesis were measured over a course of 2 years. In addition to seasonal rate
136 measurements, inhibition and stimulation experiments, stable isotope probing, and molecular
137 analysis were carried out to find out if SRZ methanogenesis 1) is controlled by environmental
138 parameters, 2) shows seasonal variability, 3) is based on non-competitive substrates with a special
139 focus on methylophilic methanogens.

140 2. Material and Methods

141 2.1 Study site

142 Samples were taken at the Time Series Station "Boknis Eck" (BE, 54°31.15 N, 10°02.18 E;
143 www.bokniseck.de) located at the entrance of Eckernförde Bay in the southwestern Baltic Sea with a
144 water depth of about 28 m (map of sampling site can be found in e.g. Hansen et al., (1999)). From
145 mid of March until mid of September the water column is strongly stratified due to the inflow of
146 saltier North Sea water and a warmer and fresher surface water (Bange et al., 2011). Organic matter
147 degradation in the deep layers causes pronounced hypoxia (March-Sept) or even anoxia
148 (August/September) (Smetacek, 1985; Smetacek et al., 1984). The source of organic material is
149 phytoplankton blooms that occur regularly in spring (February-March) and fall (September-
150 November) and are followed by pronounced sedimentation of organic matter (Bange et al., 2011). To
151 a lesser extent, phytoplankton blooms and sedimentation are also observed during the summer
152 months (July/August) (Smetacek et al., 1984). Sediments at BE are generally classified as soft, fine-
153 grained muds (< 40 µm) with a carbon content of 3 to 5 wt% (Balzer et al., 1986). The bulk of organic
154 matter in Eckernförde Bay sediments originates from marine plankton and macroalgal sources (Orsi
155 et al., 1996), and its degradation leads to production of free methane gas (Wever & Fiedler, 1995;
156 Abegg & Anderson, 1997; Wever et al., 1998). The oxygen penetration depth is limited to the upper
157 few millimeters when bottom waters are oxic (Preisler et al., 2007). Reducing conditions within the
158 sulfate reduction zone lead to a dark grey/black sediments color with a strong hydrogen sulfur odor
159 in the upper meter of the sediment and dark olive-green color the deeper sediment layers (> 1 m)
160 (Abegg & Anderson, 1997).

161 2.2 Water column and sediment sampling

162 Sampling was done on a seasonal basis during the years of 2013 and 2014. One-Day field trips with
163 either F.S. Alkor (cruise no. AL410), F.K. Littorina or F.B. Polarfuchs were conducted in March, June,
164 and September of each year. In 2013, additional sampling was conducted in November. At each
165 sampling month, water profiles of temperature, salinity, and oxygen concentration (optical sensor,
166 RINKO III, detection limit= 2 μ M) were measured with a CTD (Hydro-Bios). In addition, water samples
167 for methane concentration measurements were taken at 25 m water depth with a 6-Niskin bottle (4
168 Liter each) rosette attached to the CTD (Table 1). Complementary samples for water column
169 chlorophyll were taken at 25 m water depth with the CTD-rosette within the same months during
170 standardized monthly sampling cruises to Boknis Eck organized by GEOMAR.

171 Sediment cores were taken with a miniature multicorer (MUC, K.U.M. Kiel), holding 4 core liners
172 (length= 60 cm, diameter= 10 cm) at once. The cores had an average length of \sim 30 cm and were
173 stored at 10°C in a cold room (GEOMAR) until further processing (normally within 1-3 days after
174 sampling).

175 In September 2013, a gravity core was taken in addition to the MUC cores. The gravity core was
176 equipped with an inner plastic bag (polyethylene; diameter: 13 cm). After core recovery (330 cm
177 total length), the polyethylene bag was cut open at 12 different sampling depths resulting in intervals
178 of 30 cm and sampled directly on board for sediment porewater geochemistry (see Sect. 2.4),
179 sediment methane (see Sect. 2.5), sediment solid phase geochemistry (see Sect. 2.6), and microbial
180 rate measurements for hydrogenotrophic methanogenesis as described in section 2.8.

181 2.3 Water column parameters

182 At each sampling month, water samples for methane concentration measurements were taken at 25
183 m water depth in triplicates. Therefore, three 25 ml glass vials were filled bubble free directly after
184 CTD-rosette recovery and closed with butyl rubber stoppers. Biological activity in samples was
185 stopped by adding saturated mercury chloride solution, followed by storage at room temperature
186 until further treatment.

187 Concentrations of dissolved methane (CH₄) were determined by headspace gas chromatography as
188 described in Bange et al. (2010). Calibration for CH₄ was done by a two-point calibration with known
189 methane concentrations before the measurement of headspace gas samples, resulting in an error of
190 < 5 %.

191 Water samples for chlorophyll concentration were taken by transferring the complete water volume
192 (from 25 m water depth) from one water sampler into a 4.5 L Nalgene bottle, from which then
193 approximately 0.7-1 L (depending on the plankton content) were filtrated back in the GEOMAR
194 laboratory using GF/F filter (Whatman, 25 mm diameter, 8 μ M pores size). Dissolved chlorophyll a

195 concentrations were determined using the fluorometric method by Welschmeyer (1994) with an
196 error < 10 %.

197 2.4 Sediment porewater geochemistry

198 Porewater was extracted from sediment within 24 hours after core retrieval using nitrogen (N₂) pre-
199 flushed rhizons (0.2 µm, Rhizosphere Research Products, Seeberg-Elverfeldt et al., 2005). In MUC
200 cores, rhizons were inserted into the sediment in 2 cm intervals through pre-drilled holes in the core
201 liner. In the gravity core, rhizons were inserted into the sediment in 30 cm intervals directly after
202 retrieval.

203 Extracted porewater from MUC and gravity cores was immediately analyzed for sulfide using
204 standardized photometric methods (Grasshoff et al., 1999).

205 Sulfate concentrations were determined using ion chromatography (Methrom 761). Analytical
206 precision was < 1 % based on repeated analysis of IAPSO seawater standards (dilution series) with an
207 absolute detection limit of 1 µM corresponding to a detection limit of 30 µM for the undiluted
208 sample.

209 For analysis of dissolved inorganic carbon (DIC), 1.8 ml of porewater was transferred into a 2 ml glass
210 vial, fixed with 10 µl saturated HgCl₂ solution and crimp sealed. DIC concentration was determined
211 as CO₂ with a multi N/C 2100 analyzer (Analytik Jena) following the manufacturer's instructions.
212 Therefore, the sample was acidified with phosphoric acid and the outgassing CO₂ was measured. The
213 detection limit was 20 µM with a precision of 2-3 %.

214 2.5 Sediment methane concentrations

215 In March 2013, June 2013 and March 2014, one MUC core was sliced in 1 cm intervals until 6 cmbsf,
216 followed by 2 cm intervals until the end of the core. At the other sampling months, the MUC core
217 was sliced in 1 cm intervals until 6 cmbsf, followed by 2 cm intervals until 10 cmbsf and 5 cm intervals
218 until the end of the core.

219 Per sediment depth (in MUC and gravity cores), 2 cm⁻³ of sediment were transferred into a 10 ml-
220 glass vial containing 5 ml NaOH (2.5 %) for determination of sediment methane concentration per
221 volume of sediment. The vial was quickly closed with a butyl septum, crimp-sealed and shaken
222 thoroughly. The vials were stored upside down at room temperature until measurement via gas
223 chromatography. Therefore, 100 µl of headspace was removed from the gas vials and injected into a
224 Shimadzu gas chromatograph (GC-2014) equipped with a packed Haysep-D column and a flame
225 ionization detector. The column temperature was 80°C and the helium flow was set to 12 ml min⁻¹.
226 CH₄ concentrations were calibrated against CH₄ standards (Scotty gases). The detection limit was 0.1
227 ppm with a precision of 2 %.

228 2.6 Sediment solid phase geochemistry

229 Following the sampling for CH₄, the same cores described under section 2.5 were used for the
230 determination of the sediment solid phase geochemistry, i.e. porosity, particulate organic carbon
231 (POC) and particulate organic nitrogen (PON).

232 Sediment porosity of each sampled sediment section was determined by the weight difference of 5
233 cm⁻³ wet sediment after freeze-drying for 24 hours. Dried sediment samples were then used for
234 analysis of particulate organic carbon (POC) and particulate organic nitrogen (PON) with a Carlo-Erba
235 element analyzer (NA 1500). The detection limit for C and N analysis was < 0.1 dry weight percent (%)
236 with a precision of < 2 %.

237 2.7 Sediment methanogenesis

238 2.7.1 Methanogenesis in MUC cores

239 At each sampling month, three MUC cores were sliced in 1 cm intervals until 6 cmbsf, in 2 cm
240 intervals until 10 cmbsf, and in 5 cm intervals until the bottom of the core. Every sediment layer was
241 transferred to a separate beaker and quickly homogenized before sub-sampling. The exposure time
242 with air, i.e. oxygen, was kept to a minimum. Sediment layers were then sampled for determination
243 of net methanogenesis (defined as the sum of total methane production and consumption, including
244 all available methanogenic substrates in the sediment), hydrogenotrophic methanogenesis
245 (methanogenesis based on the substrates CO₂/H₂), and potential methanogenesis (methanogenesis
246 at ideal conditions, i.e. no lack of nutrients) as described in the following sections.

247 *Net methanogenesis*

248 Net methanogenesis was determined with sediment slurry experiments by measuring the headspace
249 methane concentration over time. Per sediment layer, triplicates of 5 cm⁻³ of sediment were
250 transferred into N₂-flushed sterile glass vials (30 ml) and mixed with 5 ml filtered bottom water. The
251 slurry was repeatedly flushed with N₂ to remove residual methane and to ensure complete anoxia.
252 Slurries were incubated in the dark at in-situ temperature, which varied at each sampling date (Table
253 1). Headspace samples (0.1 ml) were taken out every 3-4 days over a time period of 4 weeks and
254 analyzed on a Shimadzu GC-2104 gas chromatograph (see Sect. 2.5). Net methanogenesis rates were
255 determined by the linear increase of the methane concentration over time (minimum of 6 time
256 points, see also Fig. S1).

257 *Hydrogenotrophic methanogenesis*

258 To determine if hydrogenotrophic methanogenesis, i.e., methanogenesis based on the competitive
259 substrates H₂, is present in the sulfate-reducing zone, radioactive sodium bicarbonate (NaH¹⁴CO₃)
260 was added to the sediment.

261 Per sediment layer, sediment was sampled in triplicates with glass tubes (5 mL) which were closed
262 with butyl rubber stoppers on both ends according to (Treude et al. 2005). Through the stopper,
263 $\text{NaH}^{14}\text{CO}_3$ (dissolved in water, injection volume 6 μl , activity 222 kBq, specific activity = 1.85-2.22
264 GBq/mmol) was injected into each sample and incubated for three days in the dark at in-situ
265 temperature (Table 1). To stop bacterial activity, sediment was transferred into 50 ml glass-vials filled
266 with 20 ml sodium hydroxide (2.5 % w/w), closed quickly with rubber stoppers and shaken
267 thoroughly. Five controls were produced from various sediment depths by injecting the radiotracer
268 directly into the NaOH with sediment.

269 The production of ^{14}C -methane was determined with the slightly modified method by Treude et al.,
270 (2005) used for the determination of anaerobic oxidation of methane. The method was identical,
271 except no unlabeled methane was determined by gas chromatography. Instead, DIC values were
272 used to calculate hydrogenotrophic methane production.

273 *Potential methanogenesis in manipulated experiments*

274 To examine the interaction between sulfate reduction and methanogenesis, inhibition and
275 stimulation experiments were carried out. Therefore, every other sediment layer was sampled
276 resulting in the following examined six sediment layers: 0-1 cm, 2-3 cm, 4-5 cm, 6-8 cm, 10-15 cm
277 and 20-25 cm. From each layer, sediment slurries were prepared by mixing 5 ml sediment in a 1:1
278 ratio with adapted artificial seawater medium (salinity 24, Widdel & Bak, 1992) in N_2 -flushed, sterile
279 glass vials before further manipulations.

280 In total, four different treatments, each in triplicates, were prepared per depth: 1) with sulfate
281 addition (17 mM), 2) with sulfate (17 mM) and molybdate (22 mM) addition, 3) with sulfate (17 mM)
282 and 2-bromoethane-sulfonate (BES, 60 mM) addition, and 4) with sulfate (17 mM) and methanol (10
283 mM) addition. From here on, the following names are used to describe the different treatments,
284 respectively: 1) control treatment, 2) molybdate treatment, 3) BES treatment, and 4) methanol
285 treatment. Control treatments feature the natural sulfate concentrations occurring in sediments of
286 the sulfate reduction zone at the sampling site. Molybdate was used as an enzymatic inhibitor for
287 sulfate reduction (Oremland & Capone, 1988) and BES was used as an inhibitor for methanogenic
288 archaea (Hoehler et al., 1994). Methanol is a known non-competitive substrate, which is used by
289 methanogens but not by sulfate reducers (Oremland & Polcin, 1982), thus it is suitable to examine
290 non-competitive methanogenesis. Treatments were incubated similar to net methanogenesis
291 (2.7.1.1) by incubating sediment slurries at the respective in-situ temperature (Table 1) in the dark
292 for a time period of 4 weeks. Headspace samples (0.1 ml) were taken every 3-5 days over a time
293 period of 4 weeks and potential methanogenesis rates were determined by the linear increase of
294 methane concentration over time (minimum of 6 time points).

295

296 *Potential methylotrophic methanogenesis from methanol using stable isotope probing*

297 One additional experiment was conducted with sediments from September 2014 by adding ¹³C-
298 labelled methanol to investigate the production of ¹³C-labelled methane. Three cores were stored at
299 1°C after the September 2014 cruise until further processing ~ 3.5 months later. The low storage
300 temperature together with the expected oxygen depletion in the enclosed supernatant water after
301 retrieval of the cores likely led to slowed anaerobic microbial activity during storage time and
302 preserved the sediments for potential methanogenesis measurements.

303 Sediment cores were sliced in 2 cm intervals and the upper 0-2 cmbsf sediment layer of all three
304 cores was combined in a beaker and homogenized. Then, sediment slurries were prepared by mixing
305 5 cm⁻³ of sediment with 5 ml of artificial seawater medium in N₂-flushed, sterile glass vials (30 ml).

306 After this, methanol was added to the slurry with a final concentration of 10 mM (see 2.7.1.3).

307 Methanol was enriched with ¹³C-labelled methanol in a ratio of 1:1000 between ¹³C-labelled (99.9 %
308 ¹³C) and non-labelled methanol mostly consisting of ¹²C (manufacturer: Roth). In total, 54 vials were
309 prepared for nine different sampling time points during a total incubation time of 37 days. All vials
310 were incubated at 13°C (in situ temperature in September 2014) in the dark. At each sampling point,
311 six vials were stopped: one set of triplicates were used for headspace methane and carbon dioxide
312 determination and a second set of triplicates were used for porewater analysis.

313 Headspace methane and carbon dioxide concentrations (volume 100 µl) were determined on a
314 Shimadzu gas chromatograph (GC-2014) equipped with a packed Haysep-D column a flame ionization
315 detector and a methanizer. The methanizer (reduced nickel) reduces carbon dioxide with hydrogen
316 to methane at a temperature of 400°C. The column temperature was 80°C and the helium flow was
317 set to 12 ml min⁻¹. Methane concentrations (including reduced CO₂) were calibrated against methane
318 standards (Scotty gases). The detection limit was 0.1 ppm with a precision of 2 %.

319 Analyses of ¹³C/¹²C-ratios of methane and carbon dioxide were conducted after headspace
320 concentration measurements by using a continuous flow combustion gas chromatograph (Trace
321 Ultra, Thermo Scientific), which was coupled to an isotope ratio mass spectrometer (MAT253,
322 Thermo Scientific). The isotope ratios of methane and carbon dioxide given in the common delta-
323 notation (δ ¹³C in permill) are reported relative to Vienna Pee Dee Belemnite (VPDB) standard.

324 Isotope precision was +/- 0.5 ‰, when measuring near the detection limit of 10 ppm.

325 For porewater analysis of methanol concentration and isotope composition, each sediment slurry of
326 the triplicates was transferred into argon-flushed 15 ml centrifuge tubes and centrifuged for 6
327 minutes at 4500 rpm. Then 1 ml filtered (0.2 µm) porewater was transferred into N₂-flushed 2 ml
328 glass vials for methanol analysis, crimp sealed and immediately frozen at -20 °C. Methanol

329 concentrations and isotope composition were determined via high performance liquid
330 chromatography-ion ratio mass spectrometry (HPLC-IRMS, Thermo Fisher Scientific) at the MPI
331 Marburg. The detection limit was 50 μM with a precision of 0.3‰.

332 2.7.2 Methanogenesis in the gravity core

333 Ex situ hydrogenotrophic methanogenesis was determined in a gravity core taken in September 2013.
334 The pathway is thought to be the main methanogenic pathway in the sediment below the SMTZ in
335 Eckernförde Bay (Whiticar, 2002). Hydrogenotrophic methanogenesis was determined using
336 radioactive sodium bicarbonate ($\text{NaH}^{14}\text{CO}_3$). At every sampled sediment depth (12 depths in 30 cm
337 intervals), triplicate glass tubes (5 mL) were inserted directly into the sediment. Tubes were filled
338 bubble-free with sediment and closed with butyl rubber stoppers on both ends according to (Treude
339 et al. 2005). Methods following sampling were identical as described in 2.7.1.2.

340 2.8 Molecular analysis

341 During the non-labeled methanol treatment of the 0-1 cmbsf horizon from the September 2014
342 sampling (see 2.7.1.3), additional samples were prepared to detect and quantify the presence of
343 methanogens in the sediment. Therefore, additional 15 vials were prepared with addition of
344 methanol as described in 2.7.1.3 for five different time points (day 1 (= t_0), day 8, day 16, day 22, and
345 day 36) and stopped at each time point by transferring sediment from the triplicate slurries into
346 whirl-packs (Nasco), which then were immediately frozen at -20°C . DNA was extracted from ~ 500 mg
347 of sediment using the FastDNA[®] SPIN Kit for Soil (Biomedical). Quantitative real-time polymerase
348 chain reaction (qPCR) technique using TaqMan probes and TaqMan chemistry (Life Technologies) was
349 used for the detection of methanogens on a ViiA7 qPCR machine (Life Technologies). Primer and
350 Probe sets as originally published by Yu et al. (2005) were applied to quantify the orders
351 *Methanobacteriales*, *Methanosarcinales* and *Methanomicrobiales* along with the two families
352 *Methanosarcinaceae* and *Methanosaetaceae* within the order *Methanosarcinales*. In addition, a
353 universal primer set for detection of the domain *Archaea* was used (Yu et al. 2005).
354 Absolut quantification of the 16S rDNA from the groups mentioned above was performed with
355 standard dilution series. The standard concentration reached from 10^8 to 10^1 copies per μL .
356 Quantification of the standards and samples was performed in duplicates. Reaction was performed in
357 a final volume of 12.5 μL containing 0.5 μL of each Primer ($10\text{pmol } \mu\text{L}^{-1}$, MWG), 0.25 μL of the
358 respective probe ($10\text{ pmol } \mu\text{L}^{-1}$, Life Technologies), 4 μL H_2O (Roth), 6.25 μL TaqMan Universal Master
359 Mix II (Life Technologies) and 1 μL of sample or standard. Cycling conditions started with initial
360 denaturation and activation step for 10 min at 95°C , followed by 45 cycles of 95°C for 15 sec, 56°C
361 for 30 sec and 60°C for 60 sec. Non-template controls were run in duplicates with water instead of
362 DNA for all primer and probe sets, and remained without any detectable signal after 45 cycles.

363 2.9 Statistical Analysis

364 To determine possible environmental control parameters of SRZ methanogenesis, a Principle
365 Component Analysis (PCA) was applied according to the approach described in Gier et al. (2016).
366 Prior to PCA, the dataset was transformed into ranks to assure the same data dimension.
367 In total, two PCAs were conducted. The first PCA was used to test the relation of parameters in the
368 surface sediment (integrated methanogenesis (0-5 cm, $\text{mmol m}^{-2} \text{d}^{-1}$), POC content (average value
369 from 0-5 cmbsf, wt %), C/N (average value from 0-5 cmbsf, molar) and the bottom water (25 m water
370 depth) (oxygen (μM), temperature ($^{\circ}\text{C}$), salinity (PSU), chlorophyll ($\mu\text{g L}^{-1}$), methane (nM)). The
371 second PCA was applied on depth profiles of sediment SRZ methanogenesis ($\text{nmol cm}^{-3} \text{d}^{-1}$), sediment
372 depth (cm), sediment POC content (wt%), sediment C/N ratio (molar), and sampling month (one
373 value per depth profile at a specific month, the later in the year the higher the value).
374 For each PCA, biplots were produced to view data from different angles and to graphically determine
375 a potential positive, negative or zero correlation between methanogenesis rates and the tested
376 variables.

377 3. Results

378 3.1 Water column parameters

379 From March 2013 to September 2014, the water column had a pronounced temporal and spatial
380 variability of temperature, salinity, and oxygen (Fig. 2 and 3). In 2013, temperature of the upper
381 water column increased from March (1°C) to September (16°C), but decreased again in November
382 (11°C). The temperature of the lower water column increased from March 2013 (2°C) to November
383 2013 (12°C). In 2014, lowest temperatures of the upper and lower water column were reached in
384 March (4°C). Warmer temperatures of the upper water column were observed in June and
385 September (around 17°C), while the lower water column peaked in September (13°C).
386 Salinity increased over time during 2013, showing the highest salinity of the upper and lower water
387 column in November (18 and 23 PSU, respectively). In 2014, salinity of the upper water column was
388 highest in March and September (both 17 PSU), and lowest in June (13 PSU). The salinity of the lower
389 water column increased from March 2014 (21 PSU) to September 2014 (25 PSU).
390 In both years, June and September showed the most pronounced vertical gradient of temperature
391 and salinity, featuring a pycnocline at around ~ 14 m water depth.
392 Summer stratification was also seen in the O_2 profiles, which showed O_2 depleted conditions ($\text{O}_2 <$
393 $150 \mu\text{M}$) in the lower water column from June to September in both years, reaching concentrations
394 below 1- 2 μM (detection limit of CTD sensor) in September of both years (Fig. 2 and 3). The water
395 column was completely ventilated, i.e. homogenized, in March of both years with O_2 concentrations
396 of 300-400 μM down to the sea floor at about 28 m.

397

398 3.2 Sediment geochemistry in MUC cores

399 Sediment porewater and solid phase geochemistry results for the years 2013 and 2014 are shown in
400 Fig. 2 and 3, respectively.

401 Sulfate concentrations at the sediment surface ranged between 15-20 mM. Concentration decreased
402 with depth at all sampling months but was never fully depleted until the bottom of the core (18-29
403 cmbsf, between 2 and 7 mM sulfate). November 2013 showed the strongest decrease from ~20 mM
404 at the top to ~2 mM at the bottom of the core (27 cmbsf).

405 Opposite to sulfate, methane concentration increased with sediment depth in all sampling months
406 (Fig. 2 and 3). Over the course of a year (i.e. March to November in 2013, and March to September in
407 2014), maximum methane concentration increased, reaching the highest concentration in November
408 2013 (~1 mM at 26 cmbsf) and September 2014 (0.2 mM at 23 cmbsf), respectively. Simultaneously,
409 methane profiles became steeper, revealing higher methane concentrations at shallower sediment
410 depth late in the year. Magnitudes of methane concentrations were similar in the respective months
411 of 2013 and 2014.

412 In all sampling months, sulfide concentration increased with sediment depth (Fig. 2 and 3). Similar to
413 methane, sulfide profiles revealed higher sulfide concentrations at shallower sediment depth
414 together with higher peak concentrations over the course the sampled months in each sampling
415 year. Accordingly, November 2013 (10.5 mM at 15 cmbsf) and September 2014 (2.8 mM at 15
416 cmbsf) revealed the highest sulfide concentrations, respectively. September 2014 was the only
417 sampling month showing a pronounced decrease in sulfide concentration from 15 cmbsf to 21 cmbsf
418 of over 50 %.

419 DIC concentrations increased with increasing sediment depth at all sampling months. Concomitant
420 with highest sulfide concentrations, highest DIC concentration was detected in November 2013 (26
421 mM at 27 cmbsf). At the surface, DIC concentrations ranged between 2-3 mM at all sampling
422 months. In June of both years, DIC concentrations were lowest at the deepest sampled depth
423 compared to the other sampling months (16 mM in 2013, 13 mM in 2014).

424 At all sampling months, POC profiles scattered around 5 ± 0.9 wt % with depth. Only in November
425 2013, June 2014 and September 2014, POC content exceeded 5 wt % in the upper 0-1 cmbsf (5.9, 5.2
426 and 5.3 wt %, respectively) with the highest POC content in November 2013. Also in November 2013,
427 surface C/N ratio (0-1 cmbsf) of the particulate organic matter was lowest of all sampling months
428 (8.6). In general, C/N ratio increased with depth in both years with values around 9 at the surface and
429 values around 10-11 at the deepest sampled sediment depths.

430 3.3 Sediment geochemistry in gravity cores

431 Results from sediment porewater and solid phase geochemistry in the gravity core from September
432 2013 are shown in Fig. 4. Please note that the sediment depth of the gravity core was corrected by
433 comparing the sulfate concentrations at 0 cmbsf in the gravity core with the corresponding sulfate
434 concentration and depth in the MUC core from September 2013 (Fig. 2). The soft surface sediment is
435 often lost during the gravity coring procedure. Through this correction, the topmost layer of the
436 gravity core was set at a depth of 14 cmbsf.

437 Porewater sulfate concentration in the gravity core decreased with depth (i.e. below 0.1 mM at 107
438 cmbsf) and stayed below 0.1 mM until 324 cmbsf. Sulfate increased slightly (1.9 mM) at the bottom
439 of the core (345 cmbsf). In concert with sulfate, also methane, sulfide, DIC, POC and C/N profiles
440 showed distinct alteration in the profile at 345 cmbsf (see below, Fig. 4). As fluid seepage has not
441 been observed at the Boknis Eck station (Schlüter et al., 2000), these alterations could either indicate
442 a change in sediment properties or result from a sampling artifact from the penetration of seawater
443 through the core catcher into the deepest sediment layer. The latter process is, however, not
444 expected to considerably affect sediment solid phase properties (POC and C/N), and we therefore
445 dismissed this hypothesis.

446 Methane concentration increased steeply with depth reaching a maximum of 4.8 mM at 76 cmbsf.
447 Concentration stayed around 4.7 mM until 262 cmbsf, followed by a slight decrease until 324 cmbsf
448 (2.8 mM). From 324 cmbsf to 345 cmbsf methane increased again (3.4 mM).

449 Both sulfide and DIC concentrations increased with depth, showing a maximum at 45 cmbsf (~ 5mM)
450 and 345 cmbsf (~ 1mM), respectively. While sulfide decreased after 45 cmbsf to a minimum of ~ 300
451 μM at 324 cmbsf, it slightly increased again to ~1 mM at 345 cmbsf. In accordance, DIC
452 concentrations showed a distinct decrease between 324 cmbsf to 345 cmbsf (from 45 mM to 39
453 mM).

454 While POC contents varied around 5 wt % throughout the core, C/N ratio slightly increased with
455 depth, revealing the lowest ratio at the surface (~3) and the highest ratio at the bottom of the core
456 (~13). However, both POC and C/N showed a distinct increase from 324 cmbsf to 345 cmbsf.

457

458 3.4 Methanogenesis activity in MUC cores

459 3.4.1 Net methanogenesis

460 Net methanogenesis activity (calculated by the linear increase of methane over time, see Fig. S1) was
461 detected throughout the cores at all sampling months (Fig. 2 and 3). Activity measured in MUC cores
462 increased over the course of the year in 2013 and 2014 (that is: March to November in 2013 and
463 March to September in 2014) with lower rates mostly $< 0.1 \text{ nmol cm}^{-3} \text{ d}^{-1}$ in March and higher rates $>$

464 0.2 nmol cm⁻³ d⁻¹ in November 2013 and September 2014, respectively. In general, November 2013
465 revealed highest net methanogenesis rates (1.3 nmol cm⁻³ d⁻¹ at 1-2 cmbsf). Peak rates were
466 detected at the sediment surface (0-1 cmbsf) at all sampling months except for September 2013
467 where the maximum rates were situated between 10-15 cmbsf. In addition to the surface peaks, net
468 methanogenesis showed subsurface (= below 1 cmbsf until 30 cmbsf) maxima at all sampling
469 months, but with alternating depths (between 10 and 25 cmbsf).
470 Comparison of integrated net methanogenesis rates (0-25 cmbsf) revealed highest rates in
471 September and November 2013 (0.09 mmol m⁻² d⁻¹ and 0.08 mmol m⁻² d⁻¹, respectively) and lowest
472 rates in March 2014 (0.01 mmol m⁻² d⁻¹) (Fig. 5). A trend of increasing areal net methanogenesis rates
473 from March to September was observed in both years.

474 *3.4.2 Hydrogenotrophic methanogenesis*

475 Hydrogenotrophic methanogenesis activity determined by ¹⁴C-bicarbonate incubations of MUC cores
476 is shown in Fig. 2 and 3. In 2013, maximum activity ranged between 0.01-0.2 nmol cm⁻³ d⁻¹, while in
477 2014 maxima ranged only between 0.01 and 0.05 nmol cm⁻³ d⁻¹. In comparison, maximum
478 hydrogenotrophic methanogenesis was up to two orders of magnitude lower compared to net
479 methanogenesis. Only in March 2013 both activities reached a similar range.

480 Overall, hydrogenotrophic methanogenesis increased with depth in March, September, and
481 November 2013 and in March, June, and September 2014. In June 2013, activity decreased with
482 depth, showing the highest rates in the upper 0-5 cmbsf and the lowest at the deepest sampled
483 depth.

484 Concomitant with integrated net methanogenesis, integrated hydrogenotrophic methanogenesis
485 rates (0-25 cmbsf) were high in September 2013, with slightly higher rates in March 2013 (Fig. 5).
486 Lowest areal rates of hydrogenotrophic methanogenesis were seen in June of both years.

487 Hydrogenotrophic methanogenesis activity in the gravity core is shown in Fig. 4. Highest activity (~
488 0.7 nmol cm⁻³ d⁻¹) was measured at 45 cmbsf and 138 cmbsf, followed by a decrease with increasing
489 sediment depth reaching 0.01 nmol cm⁻³ d⁻¹ at the deepest sampled depth (345 cmbsf).

490 *3.4.3 Potential methanogenesis in manipulated experiments*

491 Potential methanogenesis rates in manipulated experiments included either the addition of
492 inhibitors (molybdate for inhibition of sulfate reduction or BES for inhibition of methanogenesis) or
493 the addition of a non-competitive substrate (methanol). Control treatments were run with neither
494 the addition of inhibitors nor the addition of methanol.

495 *Controls.* Potential methanogenesis activity in the control treatments was below 0.5 nmol cm⁻³ d⁻¹
496 from March 2014 to September 2014 (Fig. 6). Only in November 2013, control rates exceeded 0.5

497 nmol cm⁻³ d⁻¹ below 6 cmbsf. While rates increased with depth in November 2013 and June 2014,
498 they decreased with depth at the other two sampling months.

499 *Molybdate*. Peak potential methanogenesis rates in the molybdate treatments were found in the
500 uppermost sediment interval (0-1 cmbsf) at almost every sampling month with rates being 3-30
501 times higher compared to the control treatments (< 0.5 nmol cm⁻³ d⁻¹). In November 2013, potential
502 methanogenesis showed two maxima (0-1 and 10-15 cmbsf). Highest measured rates were found in
503 September 2014 (~6 nmol cm⁻³ d⁻¹), followed by November 2013 (~5 nmol cm⁻³ d⁻¹).

504 *BES*. Profiles of potential methanogenesis in the BES treatments were similar to the controls mostly
505 in the lower range < 0.5 nmol cm⁻³ d⁻¹. Only in November 2013 rates exceeded 0.5 nmol cm⁻³ d⁻¹.
506 Rates increased with depth at all sampling months, except for September 2014, where highest rates
507 were found at the sediment surface (0-1 cmbsf).

508 *Methanol*. At all sampling months, potential rates in the methanol treatments were three orders of
509 magnitude higher compared to the control treatments (< 0.5 nmol cm⁻³ d⁻¹). Except for November
510 2013, potential methanogenesis rates in the methanol treatments were highest in the upper 0-5
511 cmbsf and decreased with depth. In November 2013, highest rates were detected at the deepest
512 sampled depth (20-25 cmbsf).

513

514 *3.4.4 Potential methanogenesis followed by ¹³C-methanol labeling*

515 The concentration of total methanol concentrations (labeled and unlabeled) in the sediment
516 decreased sharply in the first 2 weeks from ~8 mM at day 1 to 0.5 mM at day 13 (Fig. 7). At day 17,
517 methanol was below the detection limit. In the first 2 weeks, residual methanol was enriched with
518 ¹³C, reaching ~200 ‰ at day 13.

519 Over the same time period, the methane content in the headspace increased from 2 ppmv at day 1
520 to ~ 66,000 ppmv at day 17 and stayed around that value until the end of the total incubation time
521 (until day 37) (Fig. 7). The carbon isotopic signature of methane ($\delta^{13}\text{C}_{\text{CH}_4}$) showed a clear enrichment
522 of the heavier isotope ¹³C (Table 3) from day 9 to 17 (no methane was detectable at day 1). After day
523 17, $\delta^{13}\text{C}_{\text{CH}_4}$ stayed around 13‰ until the end of the incubation. The content of CO₂ in the headspace
524 increased from ~8900 ppmv at day 1 to ~29,000 ppmv at day 20 and stayed around 30,000 ppmv
525 until the end of the incubation (Fig. 7). Please note, that the major part of CO₂ was dissolved in the
526 porewater, thus the CO₂ content in the headspace does not show the total CO₂ abundance in the
527 system. CO₂ in the headspace was enriched with ¹³C during the first 2 weeks (from -16.2 to -7.3 ‰)
528 but then stayed around -11 ‰ until the end of the incubation.

529 **3.5 Molecular analysis of benthic methanogens**

530 In September 2014, additional samples were run during the methanol treatment (see Sect. 2.7.) for
531 the detection of benthic methanogens via qPCR. The qPCR results are shown in Fig. 8. For a better

532 comparison, the microbial abundances are plotted together with the sediment methane
533 concentrations from the methanol treatment, from which the rate calculation for the methanol-
534 methanogenesis at 0-1 cmbsf was done (shown in Fig. 6).
535 Sediment methane concentrations increased over time revealing a slow increase in the first ~10 days,
536 followed by a steep increase between day 13 and day 20 and ending in a stationary phase.
537 A similar increase was seen in the abundance of total and methanogenic archaea. Total archaea
538 abundances increased sharply in the second week of the incubation reaching a maximum at day 16
539 ($\sim 5000 \cdot 10^6$ copies g^{-1}) and stayed around $3000 \cdot 10^6$ - $4000 \cdot 10^6$ copies g^{-1} over the course of the
540 incubation. Similarly, methanogenic archaea, namely the order *Methanosarcinales* and within this
541 order the family *Methanosarcinaceae*, showed a sharp increase in the first 2 weeks as well with the
542 highest abundances at day 16 ($\sim 6 \cdot 10^8$ copies g^{-1} and $\sim 1 \cdot 10^6$ copies g^{-1} , respectively). Until the end of
543 the incubation, the abundances of *Methanosarcinales* and *Methanosarcinaceae* decreased to about a
544 third of their maximum abundances ($\sim 2 \cdot 10^8$ copies g^{-1} and $\sim 0.4 \cdot 10^6$ copies g^{-1} , respectively).

545 3.6 Statistical Analysis

546 The PCA of integrated SRZ methanogenesis (0-5 cmbsf) (Fig. 10) showed a positive correlation with
547 bottom water temperature (Fig. 10a), bottom water salinity (Fig. 10a), bottom water methane (Fig.
548 10b), surface sediment POC content (0-5 cmbsf, Fig. 10c), and surface sediment C/N (0-5 cmbsf, Fig.
549 10b). A negative correlation was found with bottom water oxygen concentration (Fig. 10b). No
550 correlation was found with bottom water chlorophyll.

551 The PCA of methanogenesis depth profiles showed positive correlations with sediment depth (Fig.
552 11a) and C/N (Fig. 11b), and showed negative correlations with POC (Fig. 11a).

553

554 4. Discussion

555 4.1 Methanogenesis in the sulfate-reducing zone

556 On the basis of the results presented in Fig. 2 and 3, it is evident that methanogenesis and sulfate
557 reduction were concurrently active in the sulfate reduction zone (0-30 cmbsf) at Boknis Eck. Even
558 though sulfate reduction activity was not directly determined, the decrease in sulfate concentrations
559 with a concomitant increase in sulfide within the upper 30 cmbsf clearly indicated its presence (Fig. 2
560 and 3). Several previous studies confirmed the high activity of sulfate reduction in the surface
561 sediment of Eckernförde Bay, revealing rates up to 100 - $10,000$ $nmol\ cm^{-3}\ d^{-1}$ in the upper 25 cmbsf
562 (Treude et al., 2005a; Bertics et al., 2013; Dale et al., 2013). Microbial fermentation of organic matter
563 was probably high in the organic-rich sediments of Eckernförde Bay (POC contents of around 5 %, Fig.
564 2 and 3), providing high substrate availability and variety for methanogenesis.

565
566
567
568
569
570
571
572
573
574
575
576
577
578
579
580
581
582
583
584
585
586
587
588
589
590
591
592
593
594
595
596
597
598
599

The results of this study further identified methylotrophy to be a potentially important non-competitive methanogenic pathway in the sulfate-reducing zone. The pathway utilizes alternative substrates, such as methanol, to bypass competition with sulfate reducers for H₂ and acetate. A potential for methylotrophic methanogenesis within the sulfate-reducing zone was supported by the following observations;

- 1) Hydrogenotrophic methanogenesis was up to two orders of magnitude lower compared to net methanogenesis, resulting in insufficient rates to explain the observed net methanogenesis in the upper 0-30 cmbsf (Fig. 2 and 3). This finding points towards the presence of alternative methanogenic processes in the sulfate reduction zone, such as methylotrophic methanogenesis.
- 2) Methanogenesis increased when sulfate reduction was inhibited by molybdate, confirming the inhibitory effect of sulfate reduction on methanogenesis with competitive substrates (H₂ and acetate (Oremland & Polcin, 1982; King et al., 1983)) (Fig. 6), Consequently, usage of non-competitive substrates was preferred in sulfate reduction zone (especially in the upper 0-1 cmbsf, Fig. 6). Accordingly, hydrogenotrophic methanogenesis increased at depths where sulfate was depleted and thus the competitive situation was relieved (Fig. 4).
- 3) 3) The addition of BES did not result in the inhibition of methanogenesis, indicating the presence of unconventional methanogenic groups using non-competitive substrates (Fig. 7). The unsuccessful inhibition by BES can be explained either by incomplete inhibition or by the fact that the methanogens were insensitive to BES (Hoehler et al., 1994; Smith & Mah, 1981; Santoro & Konisky, 1987). The BES concentration applied in the present study (60 mM) has been shown to result in successful inhibition of methanogens in previous studies (Hoehler et al., 1994). Therefore, the presence of methanogens that are insensitive to BES is more likely. The insensitivity to BES in methanogens is explained by heritable changes in BES permeability or formation of BES-resistant enzymes (Smith & Mah, 1981; Santoro & Konisky, 1987). Such BES resistance was found in *Methanosarcina* mutants (Smith & Mah, 1981; Santoro & Konisky, 1987). This genus was successfully detected in our samples (for more details see point 5), and is known for mediating the methylotrophic pathway (Keltjens & Vogels, 1993), supporting our hypothesis on the utilization of non-competitive substrates by methanogens.
- 4) The addition of methanol to sulfate-rich sediments increased methanogenesis rates up to three orders of magnitude, confirming the potential of the methanogenic community to utilize non-competitive substrates especially in the 0-5 cmbsf sediment horizon (Fig. 6). At this sediment depth either the availability of non-competitive substrates, including methanol, was highest (derived from fresh organic matter), or the usage of non-competitive

600 substrates was increased due to the high competitive situation as sulfate reduction is most
601 active in the 0-5 cmbsf layer (Treude et al., 2005a; Bertics et al., 2013). It should be noted
602 that even though methanogenesis rates were calculated assuming a linear increase in
603 methane concentration over the entire incubation to make a better comparison between
604 different treatments, the methanol treatments generally showed a delayed response in
605 methane development (Fig. 8, Supplement, Fig. S2). We suggest that this delayed response
606 was a reflection of cell growth by methanogens utilizing the surplus methanol. We are
607 therefore unable to decipher whether methanol plays a major role as a substrate in the
608 Eckernförde Bay sediments compared to possible alternatives, as its concentration is
609 relatively low in the natural setting (~1 μM between 0 and 25 cmbsf, June 2014 sampling, G.-
610 C. Zhuang unpubl. data). It is conceivable that other non-competitive substrates, such as
611 methylated sulfides (e.g., dimethyl sulfide or methanethiol), are more relevant for the
612 support of SRZ methanogenesis.

- 613 5) Methylophilic methanogens of the order *Methanosarcinales* were detected in the
614 methanol-treatment (Fig. 8), confirming the presence of methanogens that utilize non-
615 competitive substrates in the natural environment (Boone et al., 1993), (Fig. 8). The delay in
616 growth of *Methanosarcinales* moreover hints towards the predominant usage of other non-
617 competitive substrates over methanol (see also point 4).
- 618 6) Stable isotope probing revealed highly ^{13}C -enriched methane produced from ^{13}C -labelled
619 methanol, furthermore confirming the potential of the methanogenic community to utilize
620 non-competitive substrates (Fig. 7). The production of both methane and CO_2 from methanol
621 has been shown previously in different strains of methylophilic methanogens (Penger et al.,
622 2012). The fast conversion of methanol to methane and CO_2 (methanol was consumed
623 completely in 17 days) is hinting towards the presence of methylophilic methanogens (e.g.
624 members of the family *Methanosarcinaceae*, which is known for the methylophilic pathway
625 (Keltjens & Vogels, 1993)). Please note, however, that the storage of the cores (3.5 months)
626 prior to sampling could have led to shifts in the microbial community and thus might not
627 reflect in-situ conditions of the original microbial community in September 2014. The delay in
628 methane production also seen in the stable isotope experiment was, however, only slightly
629 different (methane developed earlier, between day 8 and 12, data not shown) from the non-
630 labeled methanol treatment (between day 10 to 16, Fig. S2), which leads us to the
631 assumption that the storage time at 1°C did not dramatically affect the methanogen
632 community. Similar, in a previous study with arctic sediments, addition of substrates had no
633 stimulatory effect on the rate of methanogenesis or on the methanogen community
634 structure at low temperatures (5°C , (Blake et al., 2015)).

635 4.2 Environmental control of methanogenesis in the sulfate reduction zone

636 SRZ methanogenesis in Eckernförde Bay sediments showed variations throughout the sampling
637 period, which may be influenced by variable environmental factors such as temperature, salinity,
638 oxygen, and organic carbon. In the following, we will discuss the potential impact of those factors on
639 the magnitude and distribution of SRZ methanogenesis.

640 *Temperature*

641 During the sampling period, bottom water temperatures increased over the course of the year from
642 late winter (March, 3-4 °C) to autumn (November, 12°C, Fig. 2 and 3). The PCA revealed a positive
643 correlation between bottom water temperature and integrated SRZ methanogenesis (0-5 cmbsf). A
644 temperature experiment conducted with sediment from ~75 cmbsf in September 2014 within a
645 parallel study revealed a mesophilic temperature optimum of methanogenesis (20 °C, data not
646 shown). Whether methanogenesis in the sulfate reduction zone (0-30 cm) has the same physiology
647 remains speculative. However, AOM organisms, which are closely related to methanogens (Knittel &
648 Boetius, 2009), studied in the sulfate reduction zone from the same site were confirmed to have a
649 mesophilic physiology, too (Treude et al. 2005). The sum of these aspects lead us to the conceivable
650 conclusion that SRZ methanogenesis activity in the Eckernförde Bay is positively impacted by
651 temperature increases. Such a correlation between benthic methanogenesis and temperature has
652 been found in several previous studies from different environments ((Sansone & Martens, 1981; Crill
653 & Martens, 1983; Martens & Klump, 1984).

654

655 *Salinity and oxygen*

656 From March 2013 to November 2013, and from March 2014 to September 2014, salinity increased in
657 the bottom-near water (25 m) from 19 to 23 PSU and from 22 to 25 PSU (Fig. 2 and 3), respectively,
658 due the pronounced summer stratification in the water column between saline North Sea water and
659 less saline Baltic Sea water (Bange et al., 2011). The PCA detected a positive correlation between
660 integrated SRZ methanogenesis (0-5 cmbsf) and salinity in the bottom-near water (Fig. 10a). This
661 correlation can hardly be explained by salinity alone, as methanogens feature a broad salinity range
662 from freshwater to hypersaline (Zinder, 1993). More likely, salinity serves as an indicator of water-
663 column stratification, which is often correlated with low O₂ concentrations in the Eckernförde Bay
664 (Fig. S3, Bange et al., 2011; Bertics et al., 2013). Methanogenesis is sensitive to O₂ (Oremland, 1988;
665 Zinder, 1993), and hence conditions might be more favorable during hypoxic or anoxic events,
666 particular in the sediment closest to the sediment-water interface, but potentially also in deeper
667 sediment layers due to the absence of bioturbating and bioirrigating infauna (Dale et al., 2013;
668 Bertics et al., 2013), which could introduce O₂ beyond diffusive transport. Accordingly, the PCA

669 revealed a negative correlation between O₂ concentration close to the seafloor and SRZ
670 methanogenesis.

671

672 *Particulate organic carbon*

673 The supply of particulate organic carbon (POC) is one of the most important factors controlling
674 benthic heterotrophic processes, as it determines substrate availability and variety (Jørgensen,
675 2006). In Eckernförde Bay, the organic material reaching the seafloor originates mainly from
676 phytoplankton blooms in spring, summer and autumn (Bange et al., 2011). It has been estimated that
677 >50 % in spring (February/March), <25 % in summer (July/August) and >75 % in autumn
678 (September/October) of these blooms is reaching the seafloor (Smetacek et al., 1984), resulting in a
679 overall high organic carbon content of the sediment (5 wt %), which leads to high benthic microbial
680 degradation rates including sulfate reduction and methanogenesis (Whiticar, 2002; Treude et al.,
681 2005a; Bertics et al., 2013). Previous studies revealed that high organic matter availability can relieve
682 competition between sulfate reducers and methanogens in sulfate-containing, marine sediments
683 (Oremland et al., 1982; Holmer & Kristensen, 1994; Treude et al., 2009; Maltby et al., 2016).
684 To determine the effect of POC concentration and C/N ratio (the latter as a negative indicator for the
685 freshness of POC) on SRZ methanogenesis, two PCAs were conducted with a) the focus on the upper
686 0-5 cmbsf, which is directly influenced by freshly sedimented organic material from the water column
687 (Fig. 10), and b) the focus on the depth profiles throughout the sediment cores (up to 30 cmbsf) (Fig.
688 11).

689 *a) Effect of POC and C/N ratio in the upper 0-5 cmbsf*

690 For the upper 0-5 cmbsf in the sediment, a positive correlation was found between SRZ
691 methanogenesis (integrated) and POC content (averaged) (Fig. 10c), indicating that POC content is an
692 important controlling factor for methanogenesis in this layer. In support, highest bottom-near water
693 chlorophyll concentrations coincided with highest bottom-near water methane concentrations and
694 high integrated SRZ methanogenesis (0-5 cmbsf) in September 2013, probably as a result of the
695 sedimentation of the summer phytoplankton bloom (Fig. 9). Indeed, the PCA revealed a positive
696 correlation between integrated SRZ methanogenesis rates and bottom-near water methane
697 concentrations (Fig. 10b), when viewed over all investigated months. However, no correlation was
698 found between bottom water chlorophyll and integrated SRZ methanogenesis rates (Fig. 10). As seen
699 in Fig. 9, bottom-near high chlorophyll concentrations did not coincide with high bottom-near
700 methane concentration in June/September 2014. We explain this result by a time lag between
701 primary production in the water column and the export of the produced organic material to the
702 seafloor, which was probably even more delayed during stratification. Such a delay was observed in a
703 previous study (Bange et al., 2010), revealing enhanced water methane concentration close to the

704 seafloor approximately one month after the chlorophyll maximum. The C/N ratio (averaged over 0-5
705 cmbsf) also showed no correlation with integrated methanogenesis from the same depth layer (0-5
706 cmbsf), which is surprising as we expected that a higher C/N ratio, indicative for less labile organic
707 carbon, should have a negative effect on non-competitive methanogenesis. However, methanogens
708 are not able to directly use most of the labile organic matter due their inability to process large
709 molecules (more than two C-C bondings) (Zinder, 1993). Methanogens are dependent on other
710 microbial groups to degrade large organic compounds (e.g. amino acids) for them (Zinder, 1993).
711 Because of this substrate speciation and dependence, a delay between the sedimentation of fresh,
712 labile organic matter and the increase in methanogenesis can be expected, which would not be
713 captured by the applied PCA.

714 *b) Effect of POC and C/N ratio over 0-30 cmbsf*

715 In the PCA for the sediment profiles from the sulfate reduction zone (0-30 cmbsf), POC showed a
716 negative correlation with methanogenesis and sediment depth, while C/N ratio showed a positive
717 correlation with methanogenesis and sediment depth (Fig 11.). Given that POC remained basically
718 unchanged over the top 30 cmbsf, with the exemption of the topmost sediment layer, its negative
719 correlation with methanogenesis is probably solely explained by the increase of methanogenesis
720 with sediment depth, and can therefore be excluded as a major controlling factor. As sulfate in this
721 zone was likely never depleted to levels that are critically limiting sulfate reduction (lowest
722 concentration 1300 μM , compare e.g. with Treude et al., 2014) we do not expect a significant change
723 in the competition between methanogens and sulfate reducers. It is therefore more likely that the
724 progressive degradation of labile POC into dissolvable methanogenic substrates over depth and time
725 had a positive impact on methanogenesis. The C/N ratio indicates such a trend as the labile fraction
726 of POC decreased with depth.

727 **4.3 Relevance of methanogenesis in the sulfate reduction zone of Eckernförde Bay sediments**

728 The time series station Boknis Eck in Eckernförde Bay is known for being a methane source to the
729 atmosphere throughout the year due to supersaturated waters, which result from significant benthic
730 methanogenesis and emission (Bange et al., 2010). The benthic methane formation is thought to take
731 place mainly in sediments below the SMTZ (Treude et al., 2005a; Whiticar, 2002).

732 In the present study, we show that SRZ methanogenesis within the sulfate zone is present despite
733 sulfate concentrations $> 1 \text{ mM}$, a limit above which methanogenesis has been thought to be
734 negligible (Alperin et al., 1994; Hoehler et al., 1994; Burdige, 2006), and thus could contribute to
735 benthic methane emissions. In support of this hypothesis, high dissolved methane concentration in
736 the water column occurred with concomitant high SRZ methanogenesis activity (Fig. 9). However,
737 whether the observed water-column methane originated from SRZ methanogenesis or from gas
738 ebullition caused by methanogenesis below the SMTZ, or a mixture of both, remains speculative.

739 How much of the methane produced in the surface sediment is ultimately emitted into the water
740 column depends on the rate of methane consumption, i.e., aerobic and anaerobic oxidation of
741 methane in the sediment (Knittel & Boetius, 2009) (Fig. 1). In organic-rich sediments, such as in the
742 presented study, the oxygenated sediment layer is often only mm-thick, due to the high O₂ demand
743 of microorganisms during organic matter degradation (Jørgensen, 2006; Preisler et al., 2007). Thus,
744 the anaerobic oxidation of methane (AOM) might play a more important role for methane
745 consumption in the studied Eckernförde Bay sediments. In an earlier study from this site, AOM
746 activity was detected throughout the top 0-25 cmbsf, which included zones that were well above the
747 actual SMTZ (Treude et al., 2005a). But the authors concluded that methane oxidation was
748 completely fueled by methanogenesis from below sulfate penetration, as integrated AOM rates (0.8-
749 1.5 mmol m⁻² d⁻¹) were in the same range as the predicted methane flux (0.66-1.88 mmol m⁻² d⁻¹) into
750 the SMTZ.

751 Together with the data set presented here we postulate that AOM above the SMTZ (0.8 mmol m⁻² d⁻¹,
752 Treude et al., (2005a) could be partially or entirely fueled by SRZ methanogenesis. A similar close
753 coupling between methane oxidation and methanogenesis in the absence of definite methane
754 profiles was recently proposed from isotopic labeling experiments with sediments from the sulfate
755 reduction zone of the close-by Aarhus Bay, Denmark (Xiao et al., 2017). It is therefore likely that such
756 a cryptic methane cycling also occurs in the sulfate reduction zone of sediments in the Eckernförde
757 Bay. If, in an extreme scenario, SRZ methanogenesis would represent the only methane source for
758 AOM above the SMTZ, then maximum SRZ methanogenesis could be in the order of 1.6 mmol m⁻² d⁻¹
759 (1.5 mmol m⁻² d⁻¹ AOM + 0.09 mmol m⁻² d⁻¹ net SRZ methanogenesis).

760 Even though the contribution of SRZ methanogenesis to AOM above the SMTZ remains speculative, it
761 leads to the assumption that SRZ methanogenesis could play a much bigger role for benthic carbon
762 cycling in the Eckernförde Bay than previously thought. Whether SRZ methanogenesis at Eckernförde
763 Bay has the potential for the direct emission of methane into the water column goes beyond the
764 scope of this study and should be tested in the future.

765 5. Summary

766 The present study demonstrated that methanogenesis and sulfate reduction were concurrently
767 active within the sulfate-reducing zone in sediments at Boknis Eck (Eckernförde Bay, SW Baltic Sea).
768 The observed methanogenesis was probably based on non-competitive substrates due to the
769 competition with sulfate reducers for the substrates H₂ and acetate. Accordingly, members of the
770 family *Methanosarcinaceae*, which are known for methylotrophic methanogenesis, were found in the
771 sulfate reduction zone of the sediments and are likely to be responsible for the observed
772 methanogenesis with the potential use of non-competitive substrates such as methanol,
773 methylamines or methylated sulfides.

774 Potential environmental factors controlling SRZ methanogenesis are POC content, C/N ratio, oxygen,
775 and temperature, resulting in highest methanogenesis activity during the warm, stratified, and
776 hypoxic months after the late summer phytoplankton blooms.

777 This study provides new insights into the presence and seasonality of SRZ methanogenesis in coastal
778 sediments, and was able to demonstrate that the process could play an important role for the
779 methane budget and carbon cycling of Eckernförde Bay sediments, e.g., by directly fueling AOM
780 above the SMTZ.

781

782 Author Contribution

783 J.M. and T.T. designed the experiments. J.M. carried out all experiments. H.W.B. coordinated
784 measurements of water column methane and chlorophyll. C.R.L. and M.A.F. conducted molecular
785 analysis. M.S. coordinated ¹³C-Isotope measurements. J.M. prepared the manuscript with
786 contributions from all co-authors.

787 Data Availability

788 Research data for the present study can be accessed via the public data repository PANGAEA
789 (doi:10.1594/PANGAEA.873185).

790 Acknowledgements

791 We thank the captain and crew of F.S. Alkor, F.K. Littorina and F.B. Polarfuchs for field assistance. We
792 thank G. Schüssler, F. Wulff, P. Wefers, A. Petersen, M. Lange, and F. Evers for field and laboratory
793 assistance. For the geochemical analysis we want to thank B. Domeyer, A. Bleyer, U. Lomnitz, R.
794 Suhrberg, and V. Thoenissen. We thank F. Malien, X. Ma, A. Kock and T. Baustian for the O₂, CH₄, and
795 chlorophyll measurements from the regular monthly Boknis Eck sampling cruises. Further, we thank
796 R. Conrad and P. Claus at the MPI Marburg for the ¹³C-Methanol measurements. This study received
797 financial support through the Cluster of Excellence “The Future Ocean” funded by the German
798 Research Foundation, through the Sonderforschungsbereich (SFB) 754, and through a D-A-CH project
799 funded by the Swiss National Science Foundation and German Research foundation (grant no.
800 200021L_138057, 200020_159878/1). Further support was provided through the EU COST Action
801 PERGAMON (ESSEM 0902), through the BMBF project BioPara (grant no. 03SF0421B) and through
802 the EU’s H2020 program (Marie Curie grant NITROX # 704272 to CRL).

803

804

805

806 **References**

- 807 Abegg, F. & Anderson, A.L. (1997). The acoustic turbid layer in muddy sediments of Eckernförde Bay
 808 , Western Baltic : methane concentration , saturation and bubble characteristics. *Marine*
 809 *Geology*. 137. pp. 137–147.
- 810 Alperin, M.J., Albert, D.B. & Martens, C.S. (1994). Seasonal variations in production and consumption
 811 rates of dissolved organic carbon in an organic-rich coastal sediment. *Geochimica et*
 812 *Cosmochimica Acta*. 58 (22). pp. 4909–4930.
- 813 Bakker, D.E., Bange, H.W., Gruber, N., Johannessen, T., Upstill-Goddard, R.C., Borges, A.V., Delille, B.,
 814 Löscher, C.R., Naqvi, S.W.A., Omar, A.M. & Santana-Casiano-J.M. (2014). Air-sea interactions of
 815 natural long-lived greenhouse gases (CO₂, N₂O, CH₄) in a changing climate. In: P. S. Liss & M. T.
 816 Johnson (eds.). *Ocean-Atmosphere Interactions of Gases and Particles*. Heidelberg: Springer-
 817 Verlag, pp. 113–169.
- 818 Balzer, W., Pollehne, F. & Erlenkeuser, H. (1986). Cycling of Organic Carbon in a Marine Coastal
 819 System. In: P. G. Sly (ed.). *Sediments and Water Interactions*. New York, NY: Springer New York,
 820 pp. 325–330.
- 821 Bange, H.W., Bartell, U.H., Rapsomanikis, S. & Andreae, M.O. (1994). Methane in the Baltic and North
 822 Seas and a reassessment of the marine emissions of methane. *Global Biogeochemical Cycles*. 8
 823 (4). pp. 465–480.
- 824 Bange, H.W., Bergmann, K., Hansen, H.P., Kock, A., Koppe, R., Malien, F. & Ostrau, C. (2010).
 825 Dissolved methane during hypoxic events at the Boknis Eck time series station (Eckernförde
 826 Bay , SW Baltic Sea). *Biogeosciences*. 7. pp. 1279–1284.
- 827 Bange, H.W., Hansen, H.P., Malien, F., Laß, K., Karstensen, J., Petereit, C., Friedrichs, G. & Dale, A.
 828 (2011). Boknis Eck Time Series Station (SW Baltic Sea): Measurements from 1957 to 2010.
 829 *LOICZ-Affiliated Activities*. Inprint 20. pp. 16–22.
- 830 Bertics, V.J., Löscher, C.R., Salonen, I., Dale, A.W., Gier, J., Schmitz, R.A. & Treude, T. (2013).
 831 Occurrence of benthic microbial nitrogen fixation coupled to sulfate reduction in the seasonally
 832 hypoxic Eckernförde Bay, Baltic Sea. *Biogeosciences*. 10 (3). pp. 1243–1258.
- 833 Blake, L.I., Tveit, A., Øvreås, L., Head, I.M. & Gray, N.D. (2015). Response of Methanogens in Arctic
 834 Sediments to Temperature and Methanogenic Substrate Availability. *Planet. Space Sci.* 10 (6).
 835 pp. 1–18.
- 836 Buckley, D.H., Baumgartner, L.K. & Visscher, P.T. (2008). Vertical distribution of methane metabolism
 837 in microbial mats of the Great Sippewissett Salt Marsh. *Environmental microbiology*. 10 (4). pp.
 838 967–77.
- 839 Burdige, D.J. (2006). *Geochemistry of Marine Sediments*. New Jersey, U.S.A.: Princeton University
 840 Press.
- 841 Cicerone, R.J. & Oremland, R.S. (1988). Biogeochemical aspects of atmospheric methane. *Global*
 842 *Biogeochemical Cycles*. 2 (4). pp. 299–327.
- 843 Crill, P. & Martens, C. (1983). Spatial and temporal fluctuations of methane production in anoxic
 844 coastal marine sediments. *Limnology and Oceanography*. 28. pp. 1117–1130.
- 845 Crill, P.M. & Martens, C.S. (1986). Methane production from bicarbonate and acetate in an anoxic
 846 marine sediment. *Geochimica et Cosmochimica Acta*. 50. pp. 2089–2097.
- 847 Dale, a. W., Bertics, V.J., Treude, T., Sommer, S. & Wallmann, K. (2013). Modeling benthic–pelagic
 848 nutrient exchange processes and porewater distributions in a seasonally hypoxic sediment:
 849 evidence for massive phosphate release by Beggiatoa? *Biogeosciences*. 10 (2). pp. 629–651.
- 850 Denman, K.L., Brasseur, G., Chidthaisong, A., Ciais, P., Cox, P.M., Dickinson, R.E., Hauglustaine, D.,

851 Heinze, C., Holland, E., Jacob, D., Lohmann, U., Ramachandran, S., da Silva Dias, P.L., Wofsy, S.C.
852 & Zhang, X. (2007). Couplings Between Changes in the Climate System and Biogeochemistry. In:
853 S. Solomon, D. Qin, M. Manning, Z. Chen, M. Marquis, K. B. Averyt, M. Tignor, & H. L. Miller
854 (eds.). *Climate Change 2007: The Physical Science Basis. Contribution of Working Group I to the*
855 *Fourth Assessment Report of the Intergovernmental Panel on Climate Change*. Cambridge,
856 United Kingdom and New York, NY, USA: Cambridge University Press.

857 EPA (2010). *Methane and nitrous oxide emissions from natural sources*. Washington, DC, USA.

858 Ferdelman, T.G., Lee, C., Pantoja, S., Harder, J., Bebout, B.M. & Fossing, H. (1997). Sulfate reduction
859 and methanogenesis in a Thioploca-dominated sediment off the coast of Chile. *Geochimica et*
860 *Cosmochimica Acta*. 61 (15). pp. 3065–3079.

861 Gier, J., Sommer, S., Löscher, C.R., Dale, A.W., Schmitz, R.A. & Treude, T. (2016). Nitrogen fixation in
862 sediments along a depth transect through the Peruvian oxygen minimum zone. *Biogeosciences*.
863 13 (14). pp. 4065–4080.

864 Grasshoff, K., Ehrhardt, M. & Kremmling, K. (1999). *Methods of Seawater Analysis*. Weinheim: Verlag
865 Chemie.

866 Hansen, H.-P., Giesenhausen, H.C. & Behrends, G. (1999). Seasonal and long-term control of bottom-
867 water oxygen deficiency in a stratified shallow-water coastal system. *ICES Journal of Marine*
868 *Science*. 56. pp. 65–71.

869 Hartmann, D.L., Klein Tank, A.M.G., Rusticucci, M., Alexander, L.V., Brönnimann, S., Charabi, Y.,
870 Dentener, F.J., Dlugokencky, D.R., Easterling, D.R., Kaplan, A., Soden, B.J., Thorne, P.W., Wild,
871 M. & Zhai, P.M. (2013). Observations: Atmosphere and Surface. In: *Climate Change 2013: The*
872 *Physical Science Basis. Contribution Group I to the Fifth Assessment Report of the*
873 *Intergovernmental Panel on Climate Change*. United Kingdom and New York, NY, USA:
874 Cambridge University Press.

875 Hoehler, T.M., Alperin, M.J., Albert, D.B. & Martens, C.S. (1994). Field and laboratory studies of
876 methane oxidation in an anoxic marine sediment: Evidence for a methanogen-sulfate reducer
877 consortium. *Global Biogeochemical Cycles*. 8 (4). pp. 451–463.

878 Holmer, M. & Kristensen, E. (1994). Coexistence of sulfate reduction and methane production in an
879 organic-rich sediment. *Marine Ecology Progress Series*. 107. pp. 177–184.

880 Jackson, D.R., Williams, K.L., Wever, T.F., Friedrichs, C.T. & Wright, L.D. (1998). Sonar evidence for
881 methane ebullition in Eckernförde Bay. *Continental Shelf Research*. 18. pp. 1893–1915.

882 Jørgensen, B.B. (2006). Bacteria and marine Biogeochemistry. In: H. D. Schulz & M. Zabel (eds.).
883 *Marine Geochemistry*. Berlin/Heidelberg: Springer-Verlag, pp. 173–207.

884 Jørgensen, B.B. & Parkes, R.J. (2010). Role of sulfate reduction and methane production by organic
885 carbon degradation in eutrophic fjord sediments (Limfjorden, Denmark). *Limnology and*
886 *Oceanography*. 55 (3). pp. 1338–1352.

887 Keltjens, J.T. & Vogels, G.D. (1993). Conversion of methanol and methylamines to methane and
888 carbon dioxide. In: J. G. Ferry (ed.). *Methanogenesis: Ecology, Physiology, Biochemistry &*
889 *Genetics*. Chapman & Hall, pp. 253–303.

890 King, G.M., Klug, M.J. & Lovley, D.R. (1983). Metabolism of acetate, methanol, and methylated
891 amines in intertidal sediments of lowes cove, maine. *Applied and environmental microbiology*.
892 45 (6). pp. 1848–1853.

893 Knittel, K. & Boetius, A. (2009). Anaerobic oxidation of methane: progress with an unknown process.
894 *Annual review of microbiology*. 63. pp. 311–34.

895 Lennartz, S.T., Lehmann, A., Herrford, J., Malien, F., Hansen, H.-P., Biester, H. & Bange, H.W. (2014).
896 Long-term trends at the Boknis Eck time series station (Baltic Sea), 1957–2013: does climate
897 change counteract the decline in eutrophication? *Biogeosciences*. 11 (22). pp. 6323–6339.

- 898 Maltby, J., Sommer, S., Dale, A.W. & Treude, T. (2016). Microbial methanogenesis in the sulfate-
899 reducing zone of surface sediments traversing the Peruvian margin. *Biogeosciences*. 13. pp.
900 283–299.
- 901 Martens, C.S., Albert, D.B. & Alperin, M.J. (1998). Biogeochemical processes controlling methane in
902 gassy coastal sediments---Part 1 . A model coupling organic matter flux to gas production ,
903 oxidation and transport. *Continental Shelf Research*. 18. pp. 14–15.
- 904 Martens, C.S. & Klump, J. V (1984). Biogeochemical cycling in an organic-rich coastal marine basin 4.
905 An organic carbon budget for sediments dominated by sulfate reduction and methanogenesis.
906 *Geochimica et Cosmochimica Acta*. 48. pp. 1987–2004.
- 907 Naqvi, S.W. a., Bange, H.W., Fariás, L., Monteiro, P.M.S., Scranton, M.I. & Zhang, J. (2010). Marine
908 hypoxia/anoxia as a source of CH₄ and N₂O. *Biogeosciences*. 7 (7). pp. 2159–2190.
- 909 Oremland, R.S. (1988). Biogeochemistry of methanogenic bacteria. In: A. J. B. Zehnder (ed.). *Biology*
910 *of Anaerobic Microorganisms*. New York: J. Wiley & Sons, pp. 641–705.
- 911 Oremland, R.S. & Capone, D.G. (1988). Use of specific inhibitors in biogeochemistry and microbial
912 ecology. In: K. C. Marshall (ed.). *Advances in Microbial Ecology*. Advances in Microbial Ecology.
913 Boston, MA: Springer US, pp. 285–383.
- 914 Oremland, R.S., Marsh, L.M. & Polcin, S. (1982). Methane production and simultaneous sulfate
915 reduction in anoxic, salt-marsh sediments. *Nature*. 286. pp. 143–145.
- 916 Oremland, R.S. & Polcin, S. (1982). Methanogenesis and Sulfate Reduction : Competitive and
917 Noncompetitive Substrates in Estuarine Sediments. *Applied and Environmental Microbiology*. 44
918 (6). pp. 1270–1276.
- 919 Orsi, T.H., Werner, F., Milkert, D., Anderson, a. L. & Bryant, W.R. (1996). Environmental overview of
920 Eckernförde Bay, northern Germany. *Geo-Marine Letters*. 16 (3). pp. 140–147.
- 921 Penger, J., Conrad, R. & Blaser, M. (2012). Stable carbon isotope fractionation by methylotrophic
922 methanogenic archaea. *Applied and environmental microbiology*. 78 (21). pp. 7596–602.
- 923 Pimenov, N., Davidova, I., Belyaev, S., Lein, A. & Ivanov, M. (1993). Microbiological processes in
924 marine sediments in the Zaire River Delta and the Benguela upwelling region. *Geomicrobiology*
925 *Journal*. 11 (3–4). pp. 157–174.
- 926 Preisler, A., de Beer, D., Lichtschlag, A., Lavik, G., Boetius, A. & Jørgensen, B.B. (2007). Biological and
927 chemical sulfide oxidation in a Beggiatoa inhabited marine sediment. *The ISME journal*. 1 (4).
928 pp. 341–353.
- 929 Reeburgh, W. (2007). Oceanic methane biogeochemistry. *Chemical Reviews*. pp. 486–513.
- 930 Sansone, F.J. & Martens, C.S. (1981). Methane Production from Acetate and Associated Methane
931 Fluxes from Anoxic Coastal Sediments. *Science*. 211 (4483). pp. 707–709.
- 932 Santoro, N. & Konisky, J. (1987). Characterization of bromoethanesulfonate-resistant mutants of
933 *Methanococcus voltae*: Evidence of a coenzyme M transport system. *Journal of Bacteriology*.
934 169 (2). pp. 660–665.
- 935 Schlüter, M., Sauter, E., Hansen, H.-P. & Suess, E. (2000). Seasonal variations of bioirrigation in
936 coastal sediments: modelling of field data. *Geochimica et Cosmochimica Acta*. 64 (5). pp. 821–
937 834.
- 938 Seeberg-Elverfeldt, J., Schluter, M., Feseker, T. & Kolling, M. (2005). Rhizon sampling of porewaters
939 near the sediment-water interface of aquatic systems. *Limnology and Oceanography-Methods*.
940 3. pp. 361–371.
- 941 Smetacek, V. (1985). The Annual Cycle of Kiel Bight Plankton: A Long-Term Analysis. *Estuaries*. 8
942 (June). pp. 145–157.
- 943 Smetacek, V., von Bodungen, B., Knoppers, B., Peinert, R., Pollehne, F., Stegmann, P. & Zeitzschel, B.

- 944 (1984). Seasonal stages characterizing the annual cycle of an inshore pelagic system. *Rapports*
945 *et Proces-Verbaux des Reunions Conseil International pour l'Exploration de la Mer*. 186. pp.
946 126–135.
- 947 Smith, M.R. & Mah, R. a. (1981). 2-Bromoethanesulfonate: A selective agent for isolating
948 resistant *Methanosarcina* mutants. *Current Microbiology*. 6 (5). pp. 321–326.
- 949 Steinle, L., Maltby, J., Treude, T., Kock, A., Bange, H.W., Engbersen, N., Zopfi, J., Lehmann, M.F. &
950 Niemann, H. (2017). Effects of low oxygen concentrations on aerobic methane oxidation in
951 seasonally hypoxic coastal waters. *Biogeosciences*. 14 (6). pp. 1631–1645.
- 952 Thießén, O., Schmidt, M., Theilen, F., Schmitt, M. & Klein, G. (2006). Methane formation and
953 distribution of acoustic turbidity in organic-rich surface sediments in the Arkona Basin, Baltic
954 Sea. *Continental Shelf Research*. 26 (19). pp. 2469–2483.
- 955 Treude, T., Krause, S., Maltby, J., Dale, A.W., Coffin, R. & Hamdan, L.J. (2014). Sulfate reduction and
956 methane oxidation activity below the sulfate-methane transition zone in Alaskan Beaufort Sea
957 continental margin sediments: Implications for deep sulfur cycling. *Geochimica et*
958 *Cosmochimica Acta*. 144. pp. 217–237.
- 959 Treude, T., Krüger, M., Boetius, A. & Jørgensen, B.B. (2005a). Environmental control on anaerobic
960 oxidation of methane in the gassy sediments of Eckernförde Bay (German Baltic). *Limnology*
961 *and Oceanography*. 50 (6). pp. 1771–1786.
- 962 Treude, T., Niggemann, J., Kallmeyer, J., Wintersteller, P., Schubert, C.J., Boetius, A. & Jørgensen, B.B.
963 (2005b). Anaerobic oxidation of methane and sulfate reduction along the Chilean continental
964 margin. *Geochimica et Cosmochimica Acta*. 69 (11). pp. 2767–2779.
- 965 Treude, T., Smith, C.R., Wenzhöfer, F., Carney, E., Bernardino, A.F., Hannides, A.K., Krgüer, M. &
966 Boetius, A. (2009). Biogeochemistry of a deep-sea whale fall: Sulfate reduction, sulfide efflux
967 and methanogenesis. *Marine Ecology Progress Series*. 382. pp. 1–21.
- 968 Welschmeyer, N.A. (1994). Fluorometric analysis of chlorophyll a in the presence of chlorophyll b and
969 pheopigments. *Limnology and Oceanography*. 39 (8). pp. 1985–1992.
- 970 Wever, T.F., Abegg, F., Fiedler, H.M., Fechner, G. & Stender, I.H. (1998). Shallow gas in the muddy
971 sediments of Eckernförde Bay, Germany. *Continental Shelf Research*. 18. pp. 1715–1739.
- 972 Wever, T.F. & Fiedler, H.M. (1995). Variability of acoustic turbidity in Eckernförde Bay (southwest
973 Baltic Sea) related to the annual temperature cycle. *Marine Geology*. 125. pp. 21–27.
- 974 Whiticar, M.J. (2002). Diagenetic relationships of methanogenesis, nutrients, acoustic turbidity,
975 pockmarks and freshwater seepages in Eckernförde Bay. *Marine Geology*. 182. pp. 29–53.
- 976 Widdel, F. & Bak, F. (1992). Gram-Negative Mesophilic Sulfate-Reducing Bacteria. In: A. Balows, H. G.
977 Trüper, M. Dworkin, W. Harder, & K.-H. Schleifer (eds.). *The Prokaryotes*. New York, NY:
978 Springer New York, pp. 3352–3378.
- 979 Wuebbles, D.J. & Hayhoe, K. (2002). Atmospheric methane and global change. *Earth-Science Reviews*.
980 57 (3–4). pp. 177–210.
- 981 Xiao, K.Q., Beulig, F., Kjeldsen, K.U., Jørgensen, B.B. & Risgaard-Petersen, N. (2017). Concurrent
982 methane production and oxidation in surface sediment from Aarhus Bay, Denmark. *Frontiers in*
983 *Microbiology*. pp. 1–12.
- 984 Zinder, S.H. (1993). Physiological ecology of methanogens. In: J. G. Ferry (ed.). *Methanogenesis*. New
985 York, NY: Chapman & Hall, pp. 128–206.
- 986

987 **Figure Captions**

988 **Figure 1:** Overview of processes relevant for benthic methane production, consumption, and
989 emission in the Eckernförde Bay. The thickness of arrows for emissions and coupling between surface
990 processes indicates the strength of methane supply. Note that this figure combines existing
991 knowledge with results from the present study. See discussion for more details.

992 **Figure 2:** Parameters measured in the water column and sediment in the Eckernförde Bay at each
993 sampling month in the year 2013. Net methanogenesis (MG) and hydrogenotrophic (hydr.)
994 methanogenesis rates are shown in triplicates with mean (solid line).

995 **Figure 3:** Parameters measured in the water column and sediment in the Eckernförde Bay at each
996 sampling month in the year 2014. Net methanogenesis (MG) and hydrogenotrophic (hydr.)
997 methanogenesis rates are shown in triplicates with mean (solid line).

998 **Figure 4:** Parameters measured in the sediment gravity core taken in the Eckernförde Bay in
999 September 2013. Hydrogenotrophic (hydr.) methanogenesis rates are shown in triplicates with mean
1000 (solid line).

1001 **Figure 5:** Integrated net methanogenesis (MG) rates (determined by net methane production) and
1002 hydrogenotrophic MG rates (determined by radiotracer incubation) in surface sediments (0-25
1003 cmbsf) of Eckernförde Bay for different sampled time points.

1004 **Figure 6:** Potential methanogenesis rates versus sediment depth in sediment sampled in November
1005 2013, March 2014, June 2014 and September 2014. Presented are four different types of incubations
1006 (treatments): *Control* (blue symbols) is describing the treatment with sediment plus artificial
1007 seawater containing natural salinity (24 PSU) and sulfate concentrations (17 mM), *molybdate* (green
1008 symbols) is the treatment with addition of molybdate (22 mM), *BES* (purple symbols) is the
1009 treatment with 60 mM BES addition, and *methanol* (red symbols) is the treatment with addition of 10
1010 mM methanol. Shown are triplicates per depth interval and the mean as a solid line. Please note the
1011 different x-axis for the methanol treatment (red).

1012 **Figure 7:** Development of headspace gas content and isotope composition of methane (CH₄) and
1013 carbon dioxide (CO₂), and porewater methanol (CH₃OH) concentration and isotope composition
1014 during the ¹³C-labeling experiment (with sediment from the 0-2 cmbsf horizon in September 2014)
1015 with addition of ¹³C-enriched methanol (¹³C:¹²C = 1:1000). *Figure above:* Concentrations of porewater
1016 methanol (CH₃OH) and headspace content of methane (CH₄) and carbon dioxide (CO₂) over time.
1017 *Figure below:* Isotope composition of porewater CH₃OH, headspace CH₄, and headspace CO₂ over
1018 time. Shown are means (from triplicates) with standard deviation.

1019 **Figure 8:** Sediment methane concentrations (with sediment from the 0-1 cmbsf in September 2014)
1020 over time in the treatment with addition of methanol (10 mM) are shown above. Shown are triplicate
1021 values per measurement. DNA copies of *Archaea*, *Methanosarcinales* and *Methanosarcinaceae* are
1022 shown below in duplicates per measurement. Please note the secondary y-axis for
1023 *Methanosarcinales* and *Methanosarcinaceae*. More data are available for methane (determined in
1024 the gas headspace) than from DNA samples (taken from the sediment) as sample volume for
1025 molecular analyzes was limited.

1026 **Figure 9:** Temporal development of integrated net surface methanogenesis (0-5 cmbsf) in the
1027 sediment and chlorophyll (green) and methane concentrations (orange) in the bottom water (25 m).
1028 Methanogenesis (MG) rates and methane concentrations are shown in means (from triplicates) with
1029 standard deviation.

1030 **Figure 10:** Principle component analysis (PCA) from three different angles of integrated surface
1031 methanogenesis (0-5 cmbsf) and surface particulate organic carbon averaged over 0-5 cmbsf (surface
1032 sediment POC), surface C/N ratio averaged over 0-5 cmbsf (surface sediment C/N), bottom water
1033 salinity, bottom water temperature (T), bottom water methane (CH₄), bottom water oxygen (O₂), and
1034 bottom water chlorophyll. Data were transformed into ranks before analysis. a) Correlation biplot of
1035 principle components 1 and 2, b) correlation biplot of principle components 1 and 3, c) correlation
1036 biplot of principle components 2 and 3. Correlation biplots are shown in a multidimensional space
1037 with parameters shown as green lines and samples shown as black dots. Parameters pointing into
1038 the same direction are positively related; parameters pointing in the opposite direction are
1039 negatively related.

1040

1041 **Figure 11:** Principle component analysis (PCA) from two different angles of net methanogenesis
1042 depth profiles and sampling month (Month), sediment depth, depth profiles of particulate organic
1043 carbon (POC) and C/N ratio (C/N). Data was transformed into ranks before analysis. a) Correlation
1044 biplot of principle components 1 and 2, b) correlation biplot of principle components 1 and 3.
1045 Correlation biplots are shown in a multidimensional space with parameters shown as green lines and
1046 samples shown as black dots. Parameters pointing into the same direction are positively related;
1047 parameters pointing in the opposite direction are negatively related.

1048

1049

1050

1051 **Table 1:** Sampling months with bottom water (~ 2 m above seafloor) temperature (Temp.), dissolved
 1052 oxygen (O₂) and dissolved methane (CH₄) concentration

Sampling Month	Date	Instrument	Temp. (°C)	O ₂ (μM)	CH ₄ (nM)	Type of Analysis
March 2013	13.03.2013	CTD	3	340	30	WC
		MUC				All
Juni 2013	27.06.2013	CTD	6	94	125	WC
		MUC				All
September 2013	25.09.2013	CTD	10	bdl	262*	WC
		MUC				All
		GC				GC-All
November 2013	08.11.2013	CTD	12	163	13	WC
		MUC				All
March 2014	13.03.2014	CTD	4	209	41*	WC
		MUC				All
June 2014	08.06.2014	CTD	7	47	61	WC
		MUC				All
September 2014	17.09.2014	CTD	13	bdl	234	WC
		MUC				All

1053 MUC = multicorer, GC= gravity corer, CTD = CTD/Rosette, bdl= below detection limit (5μM), All = methane gas
 1054 analysis, porewater analysis, sediment geochemistry, net methanogenesis analysis, hydrogenotrophic
 1055 methanogenesis analysis, GC-All= analysis for gravity cores including methane gas analysis, porewater analysis,
 1056 sediment geochemistry, hydrogenotrophic methanogenesis analysis, WC= Water column analyses including
 1057 methane analysis, chlorophyll analysis

1058 **Concentrations from the regular monthly Boknis Eck sampling cruises on 24.09.13 and 05.03. 14 (www.bokniseck.de)

1059

1060

1061

1062

1063

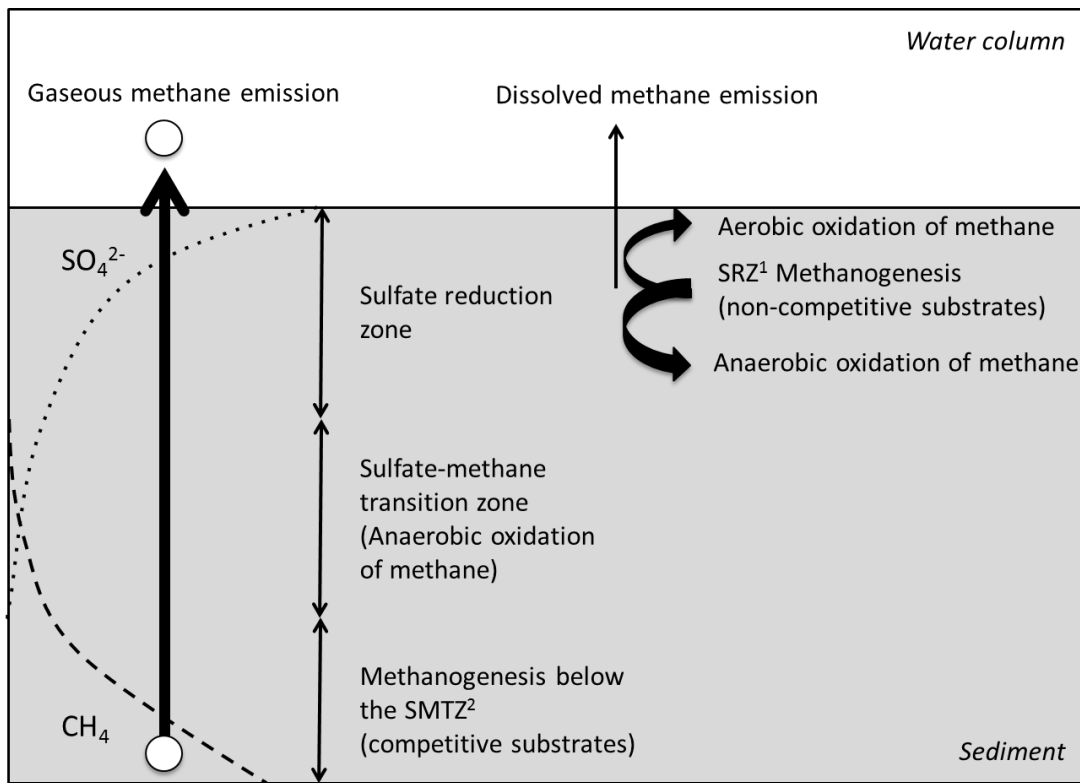
1064

1065

1066

1067 Figures

1068 Figure 1



¹ SRZ= sulfate reduction zone

² SMTZ= Sulfate-methane-transition-zone

1069

1070

1071

1072

1073

1074

1075

1076

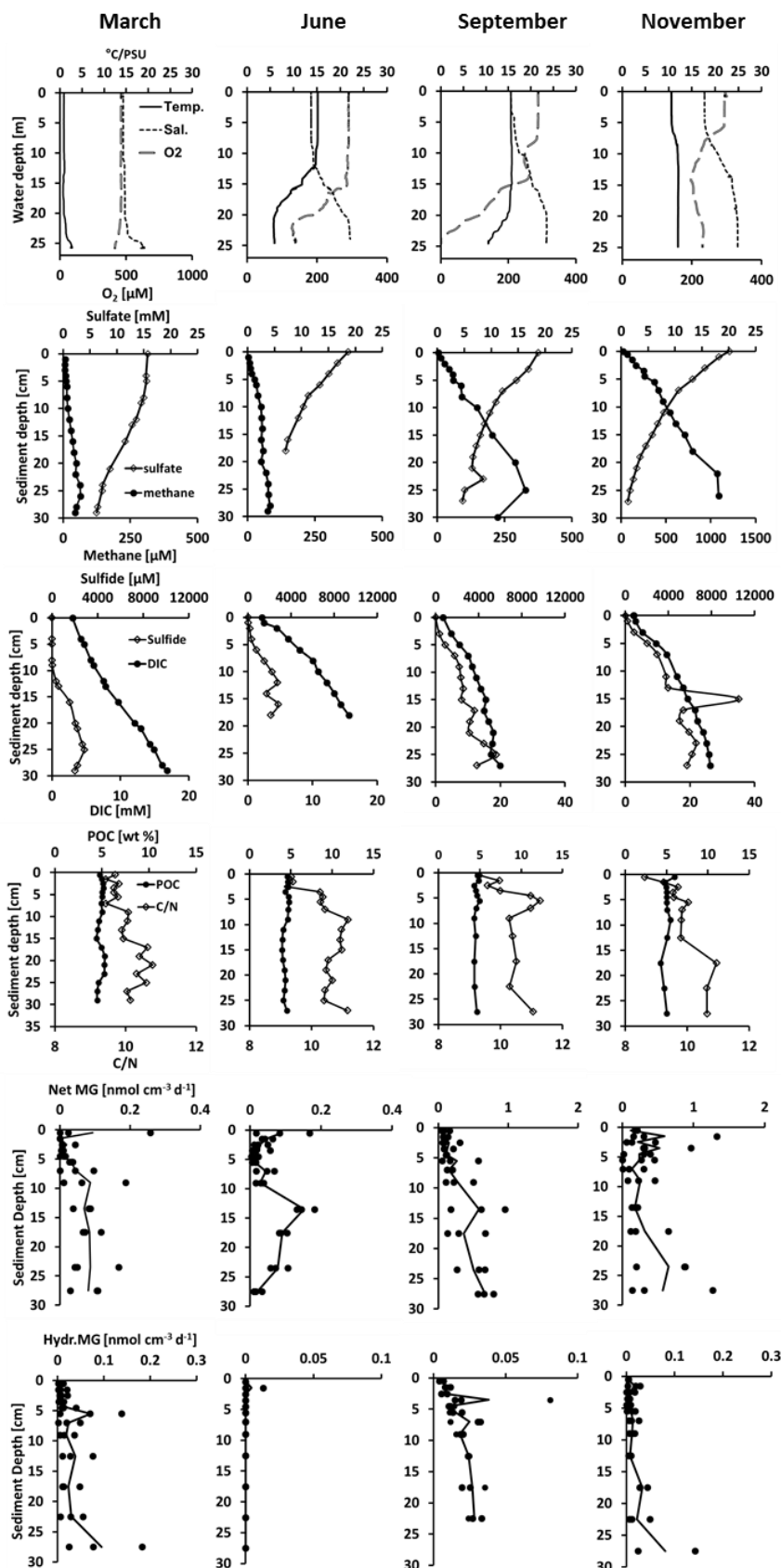
1077

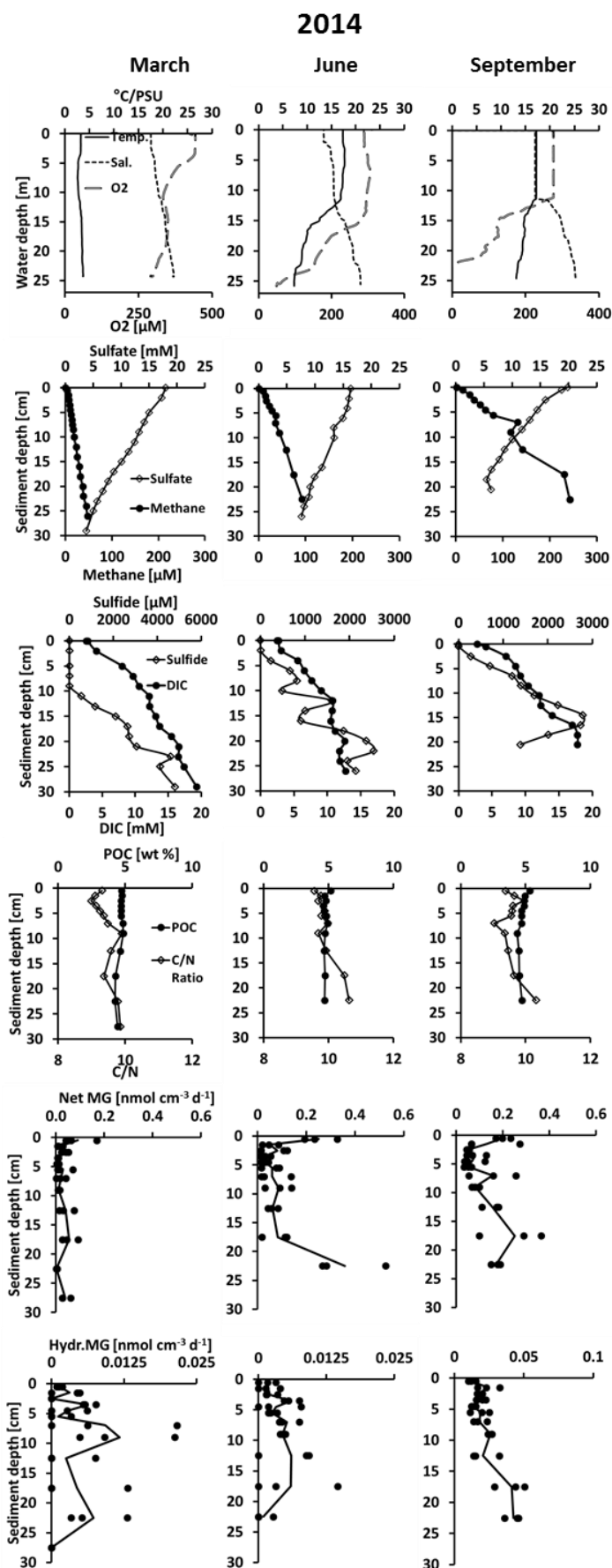
1078

1079

1080

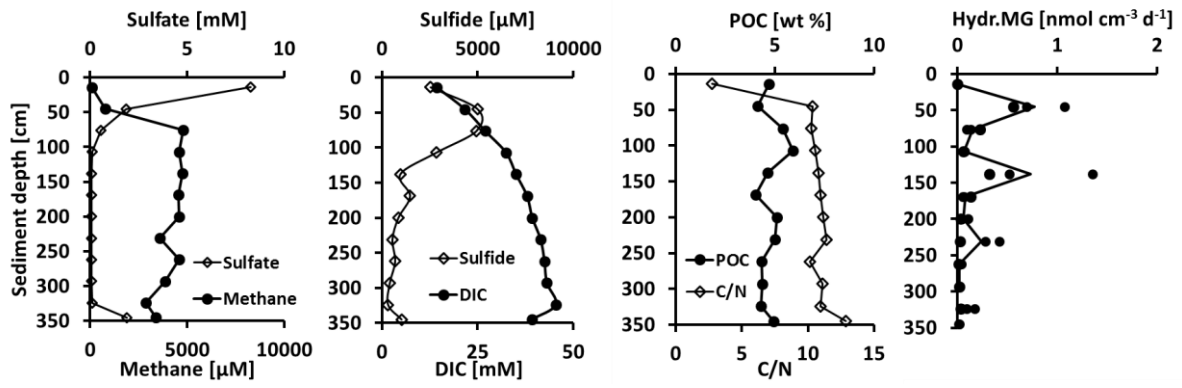
2013





1085 **Figure 4**

1086



1087

1088

1089

1090

1091

1092

1093

1094

1095

1096

1097

1098

1099

1100

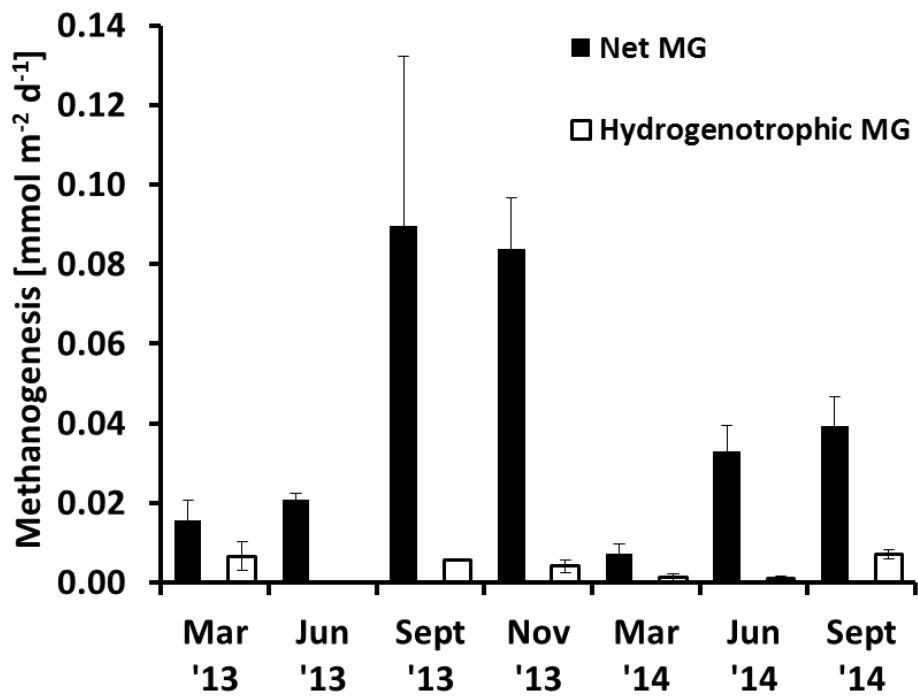
1101

1102

1103

1104 Figure 5

1105



1106

1107

1108

1109

1110

1111

1112

1113

1114

1115

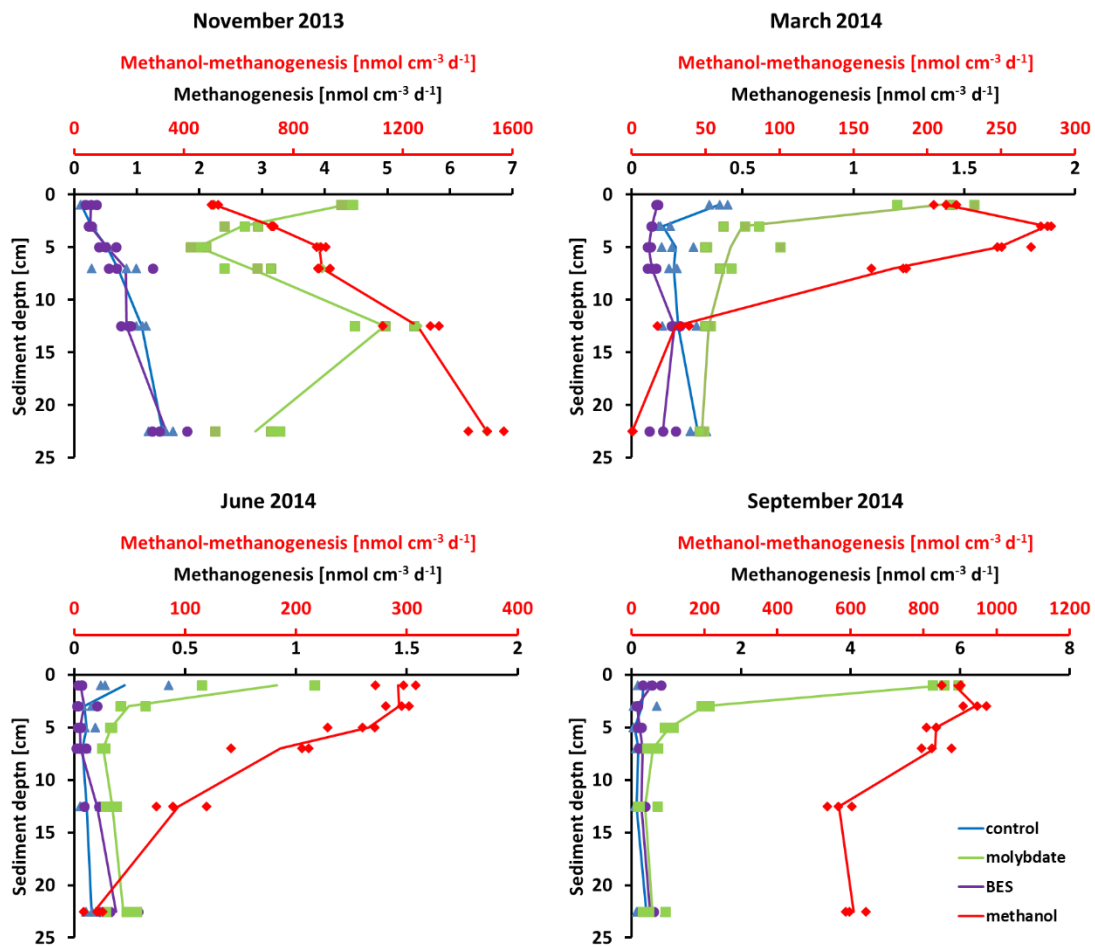
1116

1117

1118

1119 **Figure 6**

1120



1121

1122

1123

1124

1125

1126

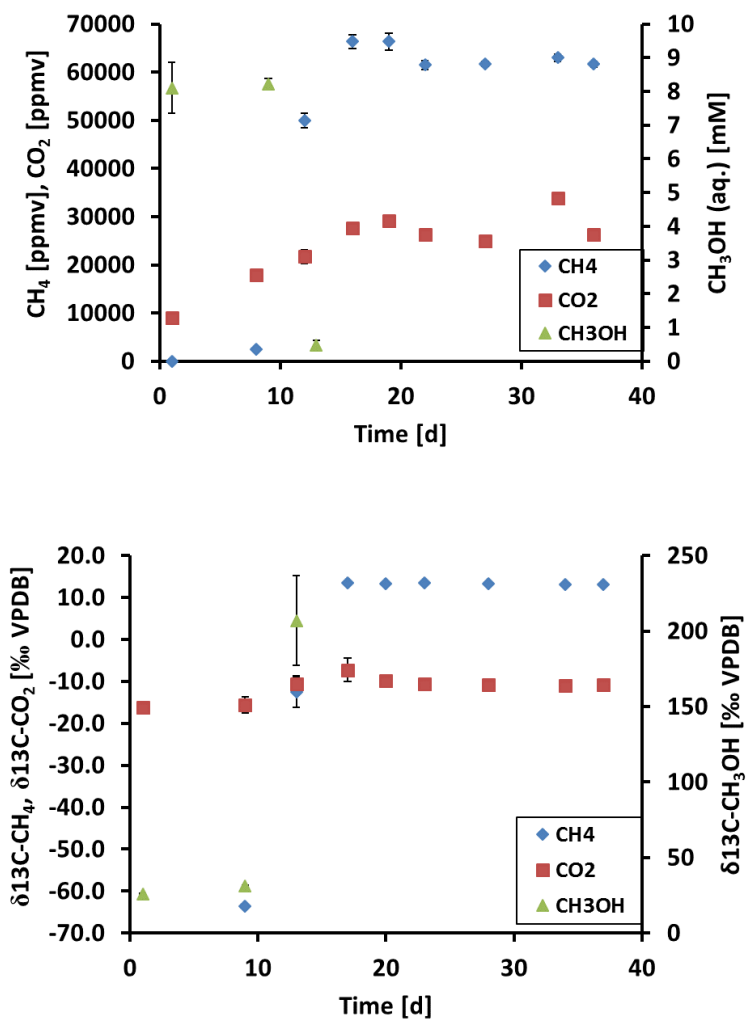
1127

1128

1129

1130

1131 Figure 7



1132

1133

1134

1135

1136

1137

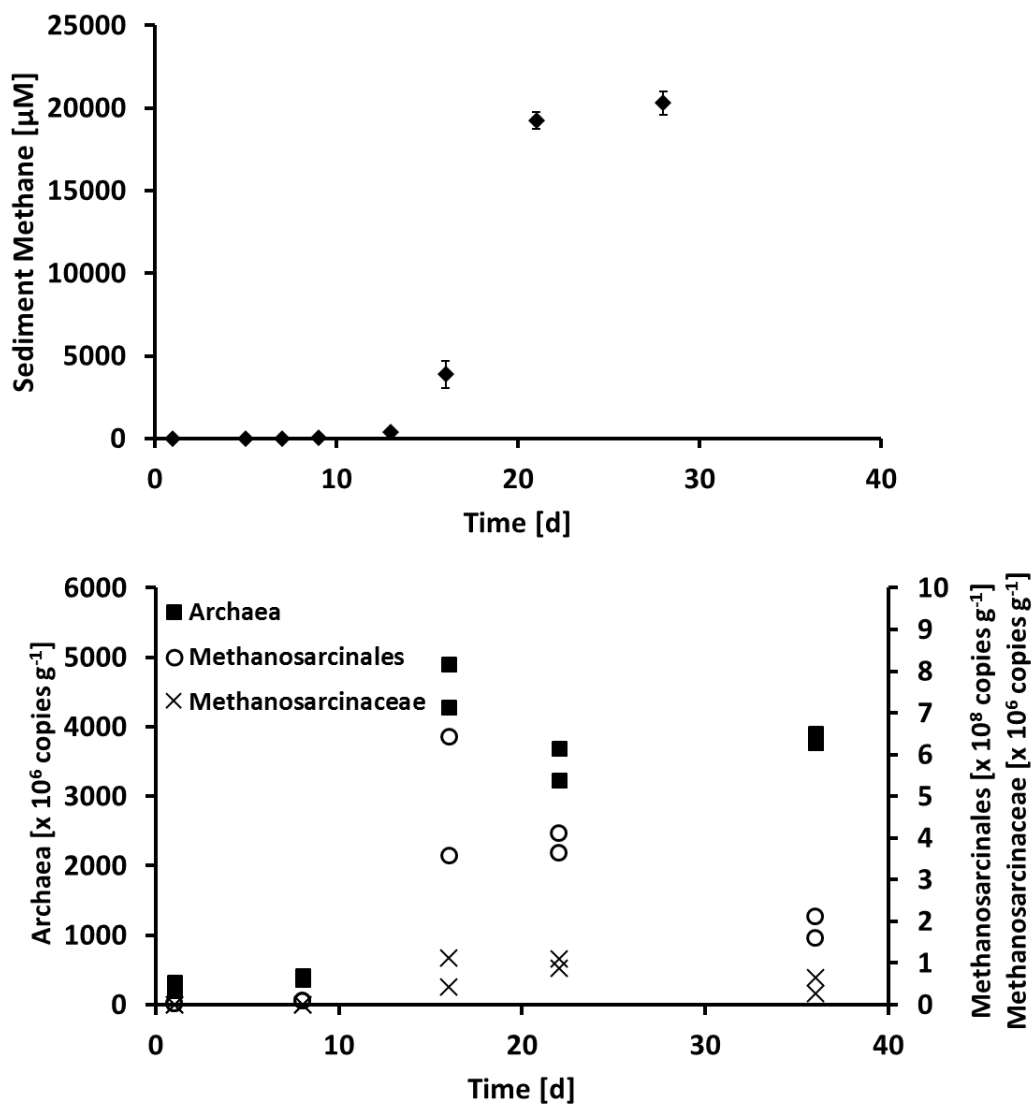
1138

1139

1140

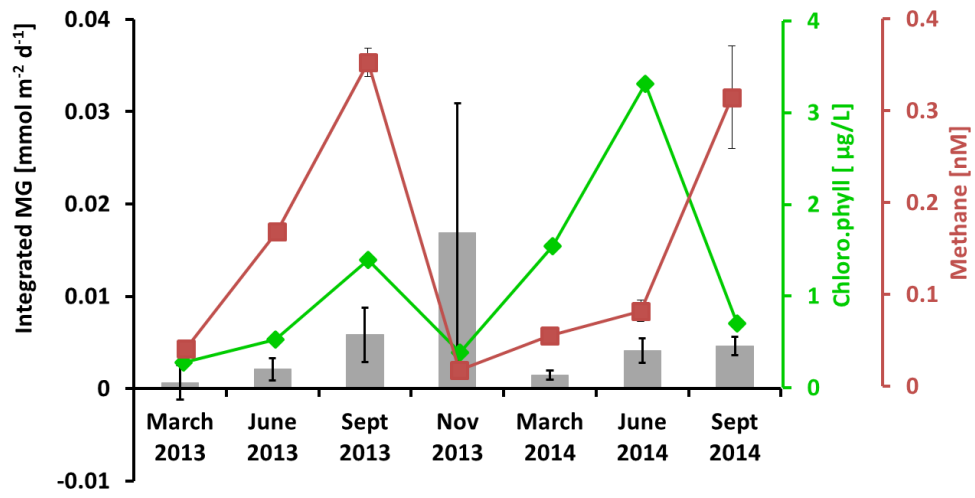
1141

1142 **Figure 8**



1143
 1144
 1145
 1146
 1147
 1148
 1149
 1150
 1151

1152 **Figure 9**



1153

1154

1155

1156

1157

1158

1159

1160

1161

1162

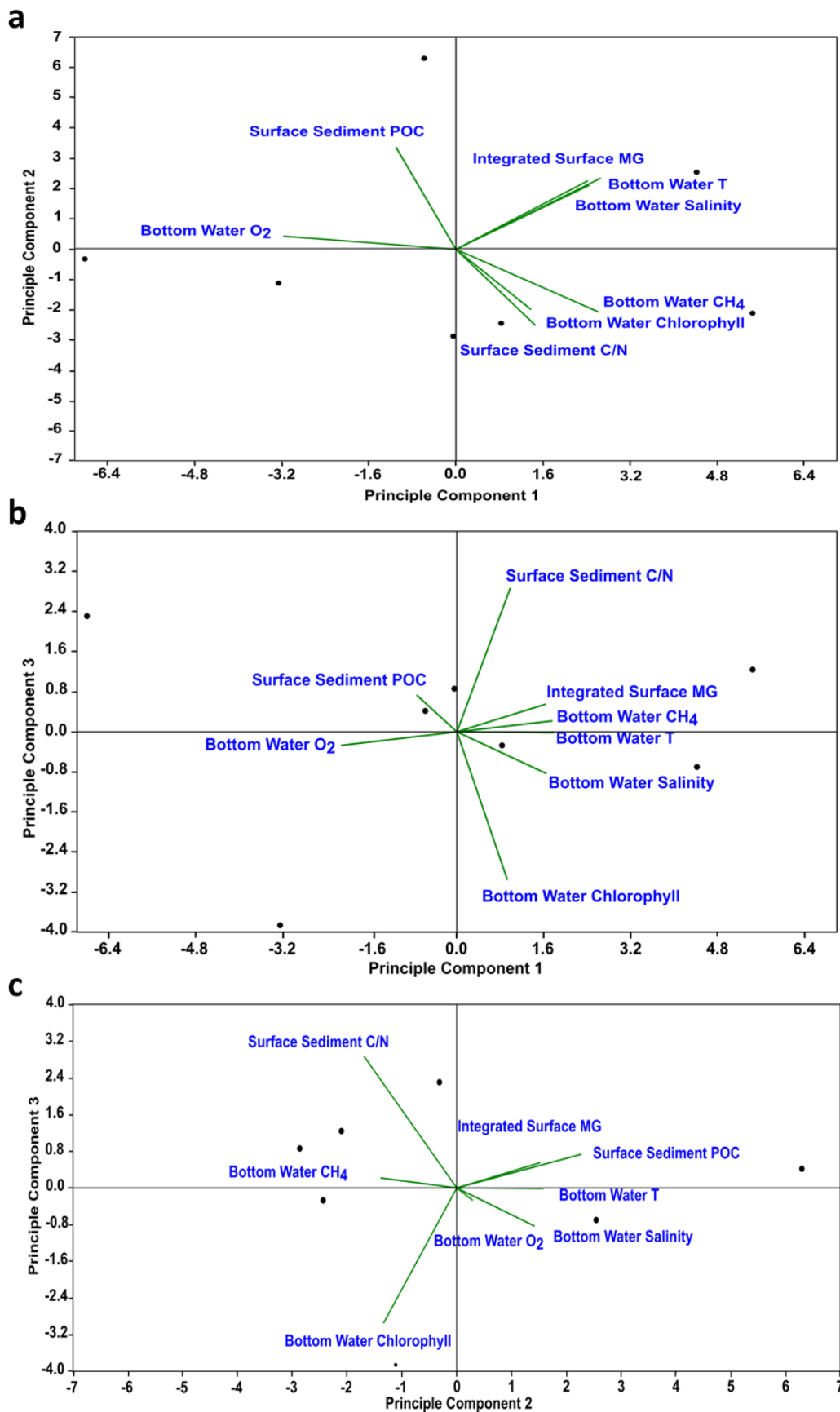
1163

1164

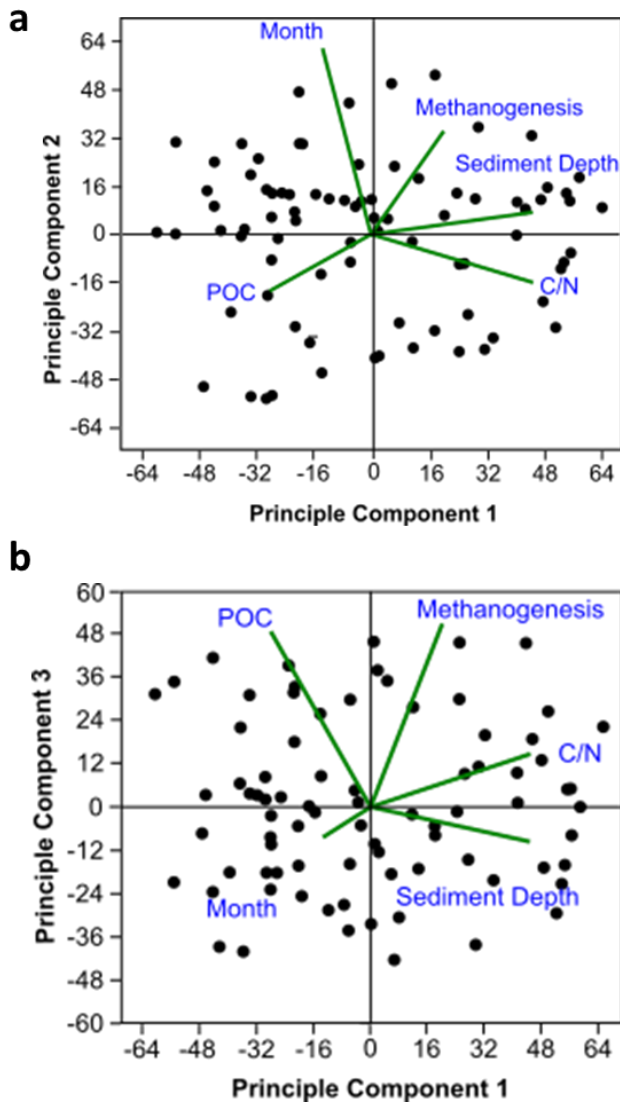
1165

1166

1167



1170 **Figure 11**



1171

1172

1173

1174

1175

1176

1177

1178